# 1. INTRODUCTION

Iscor Heavy Minerals (IHM) commissioned Iscor Consulting Services to do a feasibility study on the production of Beneficiated Titania Slag (BTS) in July 1997. BTS is a rutile substitute product that contains more than 95 % $TiO_2$. IHM's business strategy currently entails the production of a number of different products including concentrates of rutile, ilmenite, monazite and zircon as well as pig iron and titania slag from the smelting of ilmenite. BTS will be a natural addition to this product range and it will provide IHM with a premium product that is highly sought after in the market. This study was initiated as part of the feasibility study to develop a process for the production Beneficiated Titania Slag.

## 1.1 The occurrence and uses of titanium dioxide

Titanium is one of the most abundant elements in the earth's crust but deposits of titanium that are of sufficient concentration to be commercially viable are scarce (Lurie, 1987). The main ore minerals are rutile and ilmenite. Rutile is a crystalline form of titanium dioxide ($TiO_2$) and contains around 95 % $TiO_2$. Commercially viable deposits of rutile are relatively scarce. Ilmenite ($FeTiO_3$) deposits are far more abundant but they have a significantly lower $TiO_2$ content. Depending on the geological history of the deposit ores can range in composition from 40 to 80 % $TiO_2$. Most deposits being mined produce concentrates with a $TiO_2$ content between 59 and 67 %. The main impurity is iron but chromium, manganese, vanadium and magnesium can also be present among others. The ores from deposits with a $TiO_2$ content higher than 70 % are weathered ilmenites known as leucoxene. Leucoxene is exploited on a limited commercial basis. Deposits of anatase, a polymorph of rutile, have been discovered but they have not yet been commercially exploited. Other natural occurring minerals that contain titanium are brookite (rhombic $TiO_2$), perovskite ($CaTiO_3$), sphene ($CaTiSiO_5$) and geikielite ($MgTiO_3$).

The primary use of titanium is as titanium dioxide ($TiO_2$) in white pigment (Gambogi, 1991). This is used in paints, plastics and paper. Titanium dioxide pigment is superior as a white pigment due to its high refractive index and the resulting light scattering ability that provides brightness. Two pigments with a tetragonal crystal structure are produced, rutile and anatase. Rutile pigment is less reactive with other paint components when exposed to sunlight and is preferred in outdoor paints. Anatase, with a bluer tone, is used in indoor paints and paper. $TiO_2$ also finds other minor applications in welding rod coatings, in fluxes used for continuous casting of steel, in heavy aggregates and in ceramics.

## 1.2 Pigment production processes

Two processes have been developed to purify naturally occurring minerals or titaniferous slag to the required pigment purity (> 99.9 % $TiO_2$). These processes are the sulphate process and the chloride process. The sulphate process is the oldest and was developed in the 1930s while the chloride process was developed in the early 1950s.

### 1.2.1 The sulphate process

The raw materials required by this process, ilmenite or titania slag, are reacted with sulphuric acid at 150-180 °C in a batch process according to the following reaction (Gambogi, 1991):

$$5H_2O + FeTiO_3(s) + 2H_2SO_4(aq) \rightarrow FeSO_4.7H_2O(s) + TiOSO_4(aq)$$
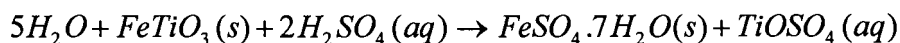
If ilmenite is used as a raw material, some ferric sulphate usually forms during leaching and this is reduced to ferrous sulphate with the addition of scrap iron. The undissolved solids are removed during clarification and the liquid is cooled and concentrated by evaporation under vacuum. Copperas ($FeSO_4.7H_2O$) is precipitated during this treatment. This part of the process is omitted when slag is used as a starting material. The concentrated solution is heated to 90 °C to hydrolyse the titanyl sulphate to insoluble titanyl hydroxide,

$$TiOSO_4(aq) + 2H_2O \rightarrow TiO(OH)_2(s) + H_2SO_4(aq)$$
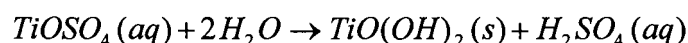
The precipitate is washed with sulphuric acid and water to remove all traces of discolouring elements such as chromium, iron, manganese and vanadium. Seed crystals are then added to ensure rutile is formed. If seed crystals are not added anatase is obtained. Finally the $TiO(OH)_2$ is calcined at 1000°C to yield $TiO_2$ pigment.

A sulphate process plant is easier to operate and maintain than a chloride process plant and it is able to use feedstock with a relatively low $TiO_2$ content. However due to the larger number of equipment pieces required the capital cost for a modern sulphate process plant can be higher than a chloride process plant of the same pigment capacity. There is also a higher volume of waste products to treat and dispose of due the use of impure feedstock and the lack of economic sulphate recycling processes. A final consideration is that rutile is insoluble in sulphuric acid. This rules out a large number of potential feedstocks (for example the various synthetic rutile products).

### 1.2.2 The chloride process

The chloride process is a modern continuous chemical process that uses a small number of complex unit operations. The feedstock to the process, high grade titania slag or rutile, is chlorinated in a fluidised-bed reactor at 925-1010 °C in the presence of coke (Bull, 1992),

$$TiO_2(s) + 2C(s) + Cl_2(g) \rightarrow 2CO(g) + TiCl_4(g)$$
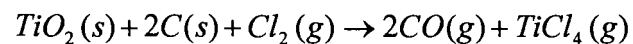
This is an exothermic reaction that sustains itself. The resulting off-gas, which contains titanium tetrachloride, is purified by distillation. The off-gas is cooled to a temperature just above the boiling point of titanium tetrachloride. Most of the chlorides with low volatilities (such as iron, chromium and manganese) condense and are removed. Titanium tetrachloride condenses during cooling and the CO and $CO_2$ gases are scrubbed before being released to the atmosphere. Some impurities, like vanadium oxychloride, are not removed during distillation. These impurities are

removed further downstream. Distillation is repeated to selectively remove chlorides with high volatilities. The purified titanium tetrachloride is oxidised to $TiO_2$ and chlorine is liberated,

$$TiCl_4(g) + O_2(g) \rightarrow TiO_2(s) + 2Cl_2(g)$$
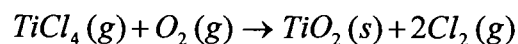
The oxidation reaction must be executed above 1000°C to produce rutile of the correct particle size distribution. It is necessary to produce a very narrow particle size distribution in the oxidation reactor to minimise sintering of particles. Growth on the walls of the reactor must also be prevented because it leads to oversized particles. Another function of the reactor is to dissipate the heat of the exothermic reaction to allow the oxidation reaction to proceed with a high efficiency.

Following oxidation, the gas is cooled and the pigment particles separated and collected. The chlorine gas is recycled to the chlorination stage and the pigment particles are forwarded to a post-treatment stage to give special properties to different grades. The post-treatment stage has recently become very important because it enhances the properties of the base pigment by surface treatment or coating processes. These processes are very complex and account for about a third of the total capital cost of a manufacturing plant.

### 1.2.3 Feedstock requirements for the chloride process

The chloride process requires feedstock with a lower impurity content than those suitable for the sulphate process. This is necessary as a result of the complex and non-selective nature of the unit processes performed at high temperatures under aggressive conditions. Table 1 summarises the impact of various feedstock impurities on the chloride process unit operations (Hollitt, 1995 and Fisher, 1997).

**Table 1.** Impact of Feedstock Impurities on Chloride Process Unit Operations

| Impurity | Impact on Chloride Process Unit Operation |
|---|---|
| FeO, MnO | Consume chlorine, coke and increase gas volumes. Form solid/liquid chloride sludge which fouls the ducting. |
| $Na_2O$, $K_2O$, CaO, MgO | Form liquid chlorides that consume coke and chlorine and defluidise the fluid bed reactor by the formation of a viscous mass that plugs the chlorinator. |
| $Al_2O_3$ | Consumes chlorine and coke, causes corrosion and forms sludge. A process step to convert Al impurities to a solid is usually included. |
| $SiO_2$ | Accumulates in the chlorinator, reducing campaign life and throughput, encourages blockages in the ducting, condenses partly with $TiCl_4$ and requires product distillation. |
| $V_2O_5$ | Follows $TiCl_4$, therefore it requires additional chemical treatment and distillation. |
| $SnO_2$ | $SnCl_4$ builds up during the oxidation step and can cause problems in the $TiCl_4$ recycle streams. Restricts sales outlets for $TiCl_4$. |
| Other heavy metal oxides | Show up in solid or liquid waste streams and create problems with economic upgrading and sale of co-products, or with their disposal in land fill sites. |
| $As_2O_5$ | Follows $TiCl_4$ and ends up in the final $TiO_2$ product, rendering the pigment unsuitable for some applications. |
| Th, Ra | Accumulate in the chlorinator brickwork and the radioactive nature causes disposal difficulties. |

The characteristics of the preferred feedstock to the chloride process can be summarised as follows (Fisher, 1997):

- TiO$_2$ content as high as possible (ideally more than 95 % TiO$_2$);
- SiO$_2$ content as low as possible (ideally none);
- Bulk density of 2.5 g/cm$^3$;
- Less than 50 ppm of uranium and thorium;
- Alkaline oxide content very low (ideally none) and;
- Heavy metals, arsenic and tin present only in trace amounts.

## 1.3 The production of titania slag

The TiO$_2$ content of ilmenite can be increased by various upgrading processes before it is used as a feedstock to one of the pigment processes. The oldest ilmenite concentration process is thermal reduction (Minckler and Baroch, 1981) and involves smelting the ilmenite ore to produce pig iron and a titanium rich slag. Smelting is currently being done by Richardsbay Minerals and Namakwa Sands in South Africa, Tinfos in Norway and Quebec Iron and Titanium (QIT) in Canada (Fisher, 1997). Titania slag produced from South African ilmenite is low in deleterious impurities and is acceptable as a feedstock to the chloride process. In contrast the slag produced from Norwegian and Canadian ilmenite has high levels of alkaline earth impurities such as Ca and Mg and is only suitable as feedstock to the sulphate process.
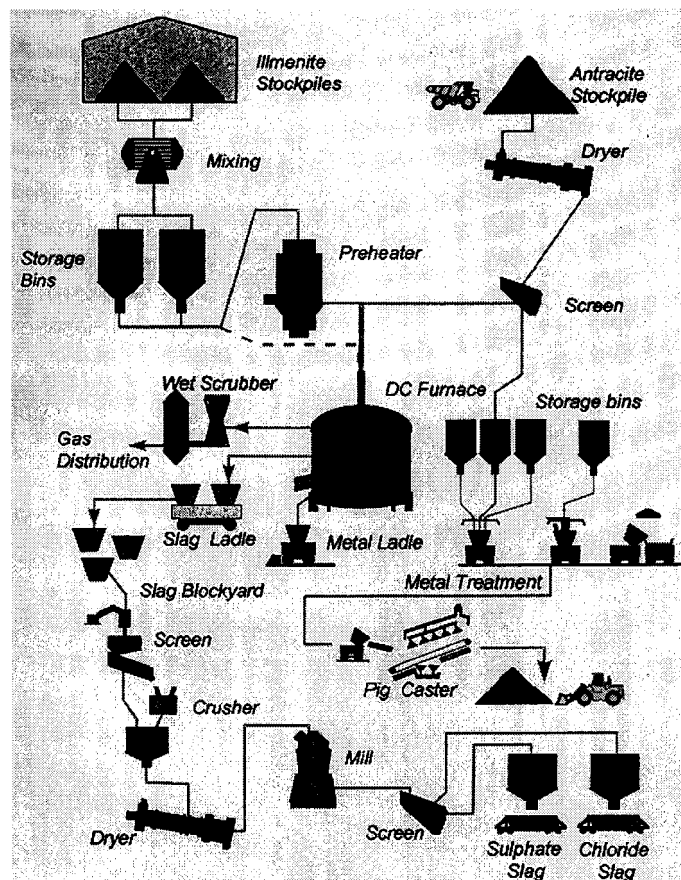


**Figure 1.** Flow diagram of the proposed IHM ilmenite smelting plant (IHM brochure, 1997).

Figure 1 shows a flow diagram of the smelting plant proposed by IHM. Ilmenite and anthracite will be fed into a 50 MVA DC plasma furnace operating at temperatures in excess of 1600 °C. Fluidity in the slag is maintained by keeping around 10 % FeO in the slag. The FeO in the slag may also have the possible additional benefit of assisting in the control of the oxygen potential in the furnace. Strongly reducing conditions will result in the undesirable reduction of $TiO_2$ to $Ti_2O_3$, $Ti_3O_5$ and even TiO. The formation of these suboxides may increase the viscosity of the slag substantially which can cause operational difficulties like frothing. Molten iron and slag will be periodically tapped from the furnace. After tapping the molten iron will be cleaned at a metal treatment station before being cast into pigs. The slag will be cast into blocks and left to cool for up to 10 days. Thereafter the slag will be crushed, dried, milled and screened to produce two size fractions. The larger fraction (+106 μm-850 μm) will be sold as feedstock to the chloride process pigment producers, while the smaller fraction (-106 μm) will be sold to sulphate process pigment producers.

## 1.4 Slag upgrading processes

Several processes have been proposed in the past to upgrade low grade titania slag to a product that is a suitable feed stock for the chloride process. The processes can be divided into the following groups:

- Oxidation and reduction roasting followed by leaching;
- Oxidation roasting followed by leaching;
- Salt roasting followed by leaching;
- Oxidation and fluxing of molten slag followed by leaching;
- Sulphation and sulphidation roasting followed by leaching and;
- Chlorination.

These processes will be discussed in more detail below.

### *1.4.1 Oxidation and reduction roasting followed by leaching*

In 1996 a plant based on oxidation and reduction roasting followed by leaching was commissioned in Canada by QIT for the upgrading of SORELSLAG™ slag (Doan, 1996). SORELSLAG™ is produced from Allard Lake ilmenite that contains relatively high levels of alkaline earth impurities such as CaO and MgO. Table 2 gives the chemical composition of SORELSLAG™ (Borowiec et al., 1996).
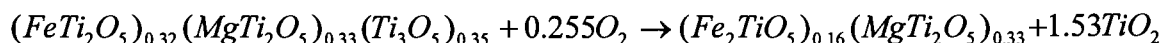
Table 2. SORELSLAG™ composition (wt %)

| TiO₂ | Fe₇ | Al₂O₃ | CaO | MgO | MnO | SiO₂ | Cr₂O₃ | V₂O₅ |
|------|-----|-------|-----|-----|-----|------|-------|------|
| 84.8 | 3.76 | 3.62 | 0.47 | 5.89 | 0.26 | 3.06 | 0.027 | 0.65 |

(* total Ti reported as $TiO_2$ regardless of valence state)

SORELSLAG™ consists mainly of the pseudobrookite solid solution with a minor amount of glassy silicate. Pseudobrookite is a solid solution of iron and titanium oxides with the general formula $M_3O_5$. The MgO impurity is present mostly in the pseudobrookite phase, while the CaO impurity occurs in the glassy silicate phase.

These phases are inherently inert toward the action of mineral acids and this makes the slag difficult to upgrade. The Upgraded Slag (UGS) process modifies the phase composition of the slag to increase the leachability of the impurities.

The first step of the process consists of sizing the slag by grinding, screening and classification to the 75-850 μm size range with a mean particle size between 250 and 350 μm. The slag is then oxidised in a fluid bed roaster at 1025 °C for 1 h. During oxidation all The Ti(III)-oxide in the slag is converted to Ti(IV)-oxide and the Fe(II) oxide is converted to Fe(III) oxide. These reactions can be represented by the following equation:

$$(FeTi_2O_5)_{0.32}(MgTi_2O_5)_{0.33}(Ti_3O_5)_{0.35} + 0.255O_2 \rightarrow (Fe_2TiO_5)_{0.16}(MgTi_2O_5)_{0.33} + 1.53TiO_2$$

The oxidation results in a major rutile ($TiO_2$) phase and a minor pseudobrookite phase ($M_3O_5$). The glassy silicate phase decomposes into wollastonite ($CaSiO_3$) and tridymite ($SiO_2$). The decomposition of the glassy silicate phase is trigged by the oxidation of FeO and can be represented by the following equation:

$$(Ca, Al, MgFe.Ti)SiO_3 + O_2 \rightarrow Fe_2O_3 + CaSiO_3 + SiO_2 + Al_2SiO_5 + TiO_2$$
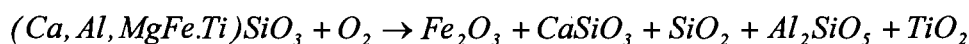
Following oxidation the slag is reduced in a fluid bed roaster at 850 °C for 1 h. Reduction of the oxidised slag takes place in two stages. In the initial stage the Fe(III) oxide is converted to Fe(II) oxide. In the second stage an MgO-enriched ilmenite-geikielite solid solution and a MgO deficient residual pseudobrookite phase and a rutile phase are formed. These changes are accompanied by the creation of a large number of pores and other defects in the crystal lattice.

Next the roasted slag is cooled before it is leached with 18-20 % HCl at 150 °C in a pressure vessel for 7 h. During leaching the impurities are removed to form soluble chlorides leaving an upgraded residue.

The leach residue is separated from the spent leach liquor, washed and calcined at 800 °C to remove moisture and residual acid. The resulting upgraded slag is a granular product with $TiO_2$ content around 95 % $TiO_2$. Table 3 gives a typical composition of UGS.

**Table 3.** Upgraded Slag composition (wt%)

| TiO₂ | FeO | Al₂O₃ | CaO | MgO | MnO | SiO₂ | Cr₂O₃ | V₂O₅ |
|------|------|------|------|------|------|------|------|------|
| 94.9 | 2.47 | 0.46 | 0.06 | 0.67 | 0.03 | 1.69 | 0.06 | 0.35 |

### 1.4.2 Oxidation roasting followed by leaching

Two processes have been proposed to upgrade titania slag by oxidation followed by leaching. In the first process (Leddy and Schecter, 1962) SORELSLAG$^{TM}$ is oxidised at 900 °C for 6 h to oxidise all the Ti(III)-oxide to Ti(IV)-oxide. The oxidised slag is then pressure leached at 200 °C in 33 % HCl for 6 h. By using this process SORELSLAG$^{TM}$ with a $TiO_2$ content of 70 % was upgraded to slag product containing 90 % $TiO_2$ and less than 0.2 % CaO and MgO. A serious disadvantage of this

process is that the feed slag has to be crushed to below 75 μm before leaching. This makes the material too fine for use in the chloride pigment process.

In second process titania slag is roasted at 800 °C - 1200 °C to oxidise the Ti(III)-oxide to Ti(IV)-oxide and the Fe(II)-oxide to Fe(III)-oxide (Tikkanen and Tholand, 1960; Tikkanen et. al., 1964). This induces cracks in the grains. The slag is then leached at 100 °C with 50 % $H_2SO_4$ in the presence of a reducing agent such as Cu for 3 h. This process has not found any commercial application due to the fact that a cost effective reducing agent still has to be found.

### 1.4.3 Salt roasting followed by leaching

QIT proposed a process for the upgrading of SORELSLAG™ based on roasting with an alkali salt followed by leaching (Jarish, 1977). Table 4 gives the composition of SORELSLAG™ used for this process.

Table 4. SORELSLAG™ composition (wt %)

| TiO₂ | FeO | Al₂O₃ | CaO | MgO | MnO | SiO₂ | Cr₂O₃ | V₂O₅ |
|---|---|---|---|---|---|---|---|---|
| 70.3 | 12.21 | 6.0 | 1.0 | 5.1 | 0.24 | 5.7 | 0.18 | 0.58 |

At first the slag is ground to –45 μm before it is mixed with an alkali salt such as NaOH in the ratio 0.3:1 to 0.6:1. The mixture is then roasted for 2 h at 900 °C. This converts most of the impurities to alkali compounds, some of which are soluble in water and others which are soluble in mineral acids. After roasting the agglomerates that formed are dispersed by wet milling for 30 min. At the same time the water soluble alkali chromate and vanadate dissolve. The remaining impurities are then removed by leaching in two stages with $H_2SO_4$. Finally the residue is separated from the spent leach solution, washed and calcined at 900 °C for 30 min. Table 5 gives the composition of the calcined slag.

Table 5. QIT salt roasting product composition (wt %)

| TiO₂ | FeO | Al₂O₃ | CaO | MgO | Na₂O | SiO₂ | Cr₂O₃ | V₂O₅ |
|---|---|---|---|---|---|---|---|---|
| 96.2 | 2.12 | 0.47 | 0.26 | 0.43 | 0.20 | 0.40 | 0.02 | 0.03 |

### 1.4.4 Oxidation and fluxing of molten slag followed by leaching

The U.S. Bureau of Mines (Elger et al., 1974) developed a modified ilmenite smelting process in the 1970s that produces a synthetic rutile product. In the first stage of the process ilmenite ore is smelted in an electric arc furnace in the presence of CaO as a fluxing agent at temperatures around 1350 °C. This results in titania slag that contains mainly pseudobrookite ($M_3O_5$) and perovskite ($CaTiO_3$) along with some glassy silicates. Table 6 gives a typical slag composition.

Table 6. U.S. Bureau of Mines slag composition (wt %)

| TiO₂ | FeO | Al₂O₃ | CaO | MgO | MnO | SiO₂ |
|---|---|---|---|---|---|---|
| 67.4 | 3.41 | 4.59 | 4.64 | 3.33 | 7.04 | 6.68 |

(* total Ti reported as $TiO_2$ regardless of valence state)

The molten slag is then oxidised before its is fluxed with a phosphate compound (for example $P_2O_5$) at around 1400 °C. After the fluxing the slag is quenched to produce a slag that consists only of rutile crystals embedded in a phosphate-rich glass phase. During the fluxing all of the impurities in the slag are partitioned to the glass phase. The glass along with the impurities is removed during an atmospheric leaching step with either $H_3PO_4$ or $H_2SO_4$. This leaves a synthetic rutile product that is a suitable feedstock for the chloride pigment process. Table 7 gives a typical composition of the final product. This process has been demonstrated on a pilot plant scale, but it is not used commercially.

**Table 7.** Synthetic rutile product composition (wt %)

| TiO₂ | FeO | Al₂O₃ | CaO | MgO | MnO | SiO₂ | P₂O₅ |
|------|------|-------|------|------|-------|------|------|
| 96.5 | 1.26 | 1.5 | 0.06 | 0.03 | 0.001 | 0.04 | 0.04 |

## 1.4.5 Sulphidation and/or sulphation roasting followed by leaching

The U.S. Bureau of Mines proposed a process for the upgrading of titania slag (Elger and Holmes, 1982) based on sulphating the impurities. The process consists of grinding the slag to below 220 μm, mixing it with $NaCO_3$ and agglomerating it with a rotating disc pelletiser. The pellets are then reacted with $SO_3$ or a mixture of $SO_2$ and $O_2$ in vertical shaft furnace at 700 °C for 7 h. This converts most of the alkaline earth oxides in the slag to sulphates. These impurities are consequently removed during a water leach procedure. The final product is suitable as feed to the chloride pigment process. Nafziger and Elger (1987) reported that this process was most successful at upgrading slag with an FeO content below 5 %. They also found that the removal of Mg and Mn was difficult and depended strongly on sufficient oxidation of the slag during roasting.

Borowiec et al. (1987) proposed a sulphiding-sulphation process for the upgrading of titania slag. Table 8. gives a typical composition of the feed slag to this process.

**Table 8.** Feed slag composition to the sulphiding-sulphation process (wt %)

| TiO₂* | FeO | Al₂O₃ | CaO | MgO | SiO₂ | Cr₂O₃ | V₂O₅ |
|-------|------|-------|------|------|------|-------|------|
| 75 | 7.6 | 1.2 | 1.0 | 4.7 | 5.3 | 0.1 | 0.3 |

(* total Ti reported as $TiO_2$ regardless of valence state)

In the first part of the process the molten slag is treated with about 5 % $Na_2S$. This produces a sulphide phase in the slag that contains most of the Fe and Mn, along with the normal pseudobrookite and glass phases. After cooling and crushing of the slag the sulphide phase is removed by leaching the slag with sulphurous acid at room temperature for 1 h. The second part of the process consists of sulphating the leached slag in a vertical tube furnace with a mixture of $SO_2$ and air at 800 °C for 4 h. During this procedure sulphates of the remaining impurities are formed. The sulphates are removed in by leaching at room temperature with water. The residual impurity content is given in Table 9.

**Table 9.** Impurity content of the residue from the sulphiding-sulphation process (wt%)

| FeO | CaO | MgO | V₂O₅ |
|------|------|------|------|
| 0.47 | 1.3 | 0.47 | 0.07 |

## 1.4.6 Chlorination

QIT proposed a process for the upgrading of titania slag based on chlorination of the impurities (Gueguin, 1986; 1990; 1991; 1995). Titania slag, containing alkaline earth impurities and some titanium as $Ti_2O_3$ (Table 10), is preheated in an inert atmosphere to 850 °C before it is contacted with chlorine gas in a fluid bed reactor.

**Table 10.** Feed slag to the chlorination process (wt %)

| TiO₂ | FeO | Al₂O₃ | CaO | MgO | MnO | SiO₂ | Cr₂O₃ | V₂O₅ |
|---|---|---|---|---|---|---|---|---|
| 81.4 | 8.97 | 2.91 | 0.20 | 5.27 | 0.27 | 1.98 | 0.18 | 0.64 |

(* total Ti reported as $TiO_2$ regardless of valence state)

The reaction of $Ti_2O_3$ with the chlorine and the impurities is an exothermic reaction that lowers the energy cost required for the chlorination reaction. During chlorination the iron and other impurities are distilled as chlorides. After chlorination the product is cooled to room temperature. The resulting product has a porous texture and consists mainly of rutile along with small amounts of aluminium and magnesium titanates. The titanates are removed by leaching the chlorinated slag with 33 % HCl at 210 °C for 4 h. Table 11 gives the final product composition.

**Table 11.** Chlorination process product composition (wt %)

| TiO₂ | FeO | Al₂O₃ | CaO | MgO | MnO | SiO₂ | Cr₂O₃ | V₂O₅ |
|---|---|---|---|---|---|---|---|---|
| 96.4 | 0.45 | 1.02 | 0.07 | 0.51 | 0.04 | 0.78 | 0.07 | 0.29 |

## 1.5 The motivation for upgrading chloride grade titania slag

All the known slag upgrading processes have as their aim the upgrading of sulphate grade titania slag to chloride grade titania slag for economic and environmental reasons. The main reason for upgrading chloride grade titania slag to a synthetic rutile product (as proposed here) is also an economic one. Figure 2 gives the 1997 prices for titaniferous feedstocks (Gambogi, 1998).
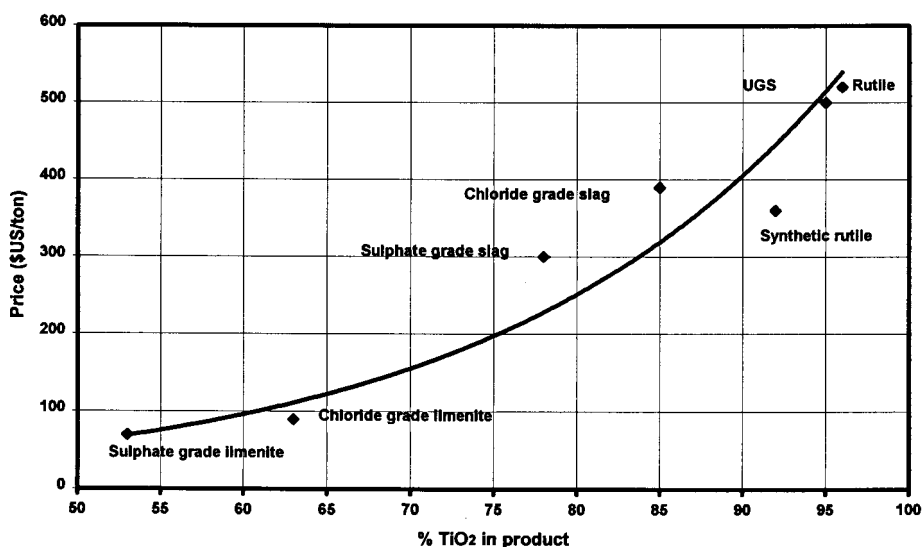


**Figure 2.** Titaniferous feedstock prices

There is a $ 110 price difference between the price of chloride grade slag (85 % $TiO_2$) and UGS (95 % $TiO_2$). The reason for this price difference can be related to the quantity of effluent generated by the chloride process when these feedstocks are used. A higher purity feedstock generates less waste and this makes it easier to comply with environmental regulations. Based on this analysis there appears to be a need for a chloride grade slag upgrading process. This study reports on the development of such a process.

# 2. PRELIMINARY INVESTIGATION

Several possible process routes for the production of beneficiated titania slag were identified in the previous chapter. All of these processes were however designed to upgrade sulphate grade titania slag. The aim of the investigation reported in this chapter was to determine the potential of some of these processes in upgrading chloride grade titania slag. The main difference between chloride and sulphate grade slag is the levels of alkaline earth elements that are present. In chloride grade slag the % MgO + % CaO < 1.2, while it exceeds 6% in sulphate grade slag (Borowiec et al., 1996). Special emphasis was placed on slag preparation and slag pre-treatment procedures.

## 2.1 Experimental design

### 2.1.1 Feed material and experimental plan

The slags used for this investigation were obtained from the $5^{th}$ IHM plasma furnace campaign (conducted in a 3MVA pilot scale furnace) of July 1996. The complete slag analyses are listed in Appendix I. Table 12 gives the concentration of selected elements in the feed slags.

**Table 12.** Chemical composition of the feed slags (wt %)

| Reference no. | Classification | $TiO_2^*$ | FeO | $P_2O_5$ |
|---|---|---|---|---|
| YS3812 | Standard slag: As-cast | 87.7 | 10.04 | - |
| YS17 | Standard slag: Granulated | 83.0 | 10.66 | - |
| YS16 | High iron slag: Granulated | 72.5 | 18.27 | - |
| YS3813 | Standard slag: Oxidised in the solid state | 85.1 | 10.66 | - |
| YS13 | High iron slag: Oxidised in the solid state | 78.3 | 16.60 | - |
| - | Standard slag: Oxidised in the molten state | 80.1 | 15.31 | - |
| - | High iron slag: Oxidised in the molten state | 74.6 | 21.61 | - |
| - | Standard slag: Phosphate treated | 69.5 | 8.83 | 7.74 |
| - | Standard slag: Oxidised en reduced | 88.1 | 8.75 | - |

*\* Ti is reported as total $TiO_2$ regardless of oxidation state*

As-cast titania slag contains mainly oxides of titanium and iron. Titanium is present in the Ti(III) and the Ti(IV) oxidation states and iron is present in the Fe(II) oxidation state. Slags subjected to various pre-treatments were chosen for this investigation. This was done to investigate the effect of slag pre-treatment on the leachability of impurities from the slag. Another important variable that was identified was the FeO content of the slag. Slags with high FeO levels can be produced with a lower energy input to the smelting furnace. This may be a process advantage and feed slags with high and low FeO contents were therefore evaluated. The effects of the various slag pre-treatment procedures on the leachability of impurities from the slag were evaluated by leaching most of the materials in hydrochloric and sulphuric acid. The phosphate treated slag was leached in hydrochloric acid, sulphuric acid and phosphoric acid, while the oxidised and reduced slag was only leached in hydrochloric acid. The increase in $TiO_2$ content of the leach residues compared to the feed was used to evaluate the effectiveness of the upgrading procedures.

## 2.2 Experimental procedure

### 2.2.1 Slag pretreatment

The standard as-cast slag (YS3812) was produced by smelting ilmenite in the presence of carbon in a 3 MVA plasma furnace. An as-cast slag block was crushed and screened to the +106-850 μm range.

The two granulated slag samples (YS16 and YS17) were produced from molten titania slag with an air granulator. These samples were also screened to the +106-850 μm size range.

Two samples of slag were produced to imitate slag that had been oxidised in the molten state; slag samples were melted in a tundish and oxidised by blowing oxygen through the molten charge with a steel lance.

Two sized slag samples (YS3813 and YS13) were oxidised in a vertical thermogravimetric furnace for 2 h at 800°C with air. The roasted product was cooled inside the furnace without any gas circulation.

The phosphate treated slag was produced by grinding 8260 g slag, 330 g lime and 1410 g ammonium phosphate in a rotating mill for 2 h. Alumina crucibles, charged with this mixture of fine material, were loaded into a muffle furnace and heated to 1300 °C. The crucibles were held at this temperature for 12 h while oxygen was circulated through the furnace. After fluxing the furnace was opened and the crucibles and their content allowed to cool rapidly in air. The solidified mass was removed from the crucible and crushed and sized to +106-850 μm prior to leaching.

The oxidised and reduced slag was produced by charging a 1000 g batch of sized slag to a Linn rotating furnace equipped with external heating and a tube with lifter bars. The slag was heated to 850 °C and held at this temperature for 2 h while air flowed through the furnace at a rate of 67.2 L/min; the gas flow was changed to a mixture of carbon monoxide and nitrogen at a rate of 11.8 and 42.5 L/min respectively for a period of 20 min prior to cooling the slag down under nitrogen flow. A second run was performed using the same procedure but using a gas mixture consisting of 67 % CO and 33 % $CO_2$ for the 20 min reducing part of the cycle.

### 2.2.2 Leaching

Most of the leach experiments were conducted in 2 L batch stirred tank reactors. The reactors were placed in thermostatically controlled water baths at 95°C. The glass reactors were closed and equipped with condensers to limit evaporation losses. Stirring at 500 rpm was provided by flat paddle type impellers driven by overhead motors and the reactors were equipped with 4 baffles each. Each reactor was filled with 1 L solution and once the reactor stabilised at the desired temperature 500 g dry feed material was charged. 20 % Hydrochloric acid, 26 % sulphuric acid and 18 % phosphoric acid solutions were respectively used for the various experiments. 20 mL Pulp samples were taken at 0; ½; 1; 2 and 4 h. These samples were filtered immediately and the filtrate was saved for chemical analysis. At the start and end of

an experiment the reactor and its contents were weighed to determine the total mass loss due to sampling and evaporation. At the end of the leach the slurry was filtered and repeatedly repulped and washed until the pH of the wash water was neutral. Special care was taken to limit losses of solids during the bulk filtration and washing operations. The washed filter cake was dried overnight at 120 °C, weighed and sampled for full chemical analysis. Solution samples were analysed by ICP-AES to determine the concentrations of respectively: Ti, Fe, Mg, Al, Mn, Cr, Ca, Si and V and by acid titration to determine the free acid concentrations. The solid samples were analysed by ICP-AES to determine the concentrations of respectively: Ti, Fe, Mg, Al, Mn, Cr, Ca, Si, V and P in the feed material and the washed leach residues.

The oxidised and reduced slag was leached in a 2 L Erlenmeyer flask fitted with a reflux condensor to limit evaporation losses. The reactor was place on a hot plate that kept the leach solution at boiling point. 20% Hydrochloric acid was used to leach the slag for up to six hours. The rest of the procedure was similar to the experiments conducted in the water bath.

## 2.3 Results and discussion

The effect of the different slag pre-treatments on slag leachability is presented in Table 13. It shows the chemical analysis of the feed materials as well as the chemical analysis of the residues after leaching in hydrochloric and sulphuric acid. The log sheets for the experiments are listed in Appendix II.

**Table 13.** The effect of different pre-treatments and slag compositions on the leachability of impurities

| Chemical composition (wt-%) | | $TiO_2$ | $FeO$ | $MgO$ | $CaO$ | $SiO_2$ |
|---|---|---|---|---|---|---|
| Standard slag: As-cast | Feed | 87.7 | 10.05 | 0.93 | 0.13 | 1.47 |
| | HCl leach residue | 88.4 | 9.08 | 0.98 | 0.10 | 1.26 |
| | $H_2SO_4$ leach residue | 88.0 | 8.95 | 0.97 | 0.10 | 1.26 |
| Standard slag: Granulated | Feed | 83.0 | 10.66 | 1.90 | 0.34 | 1.73 |
| | HCl leach residue | 84.9 | 9.85 | 1.83 | 0.17 | 1.61 |
| | $H_2SO_4$ leach residue | 84.1 | 10.05 | 1.90 | 0.19 | 1.60 |
| High iron slag: Granulated | Feed | 72.5 | 18.27 | 1.84 | 0.99 | 2.11 |
| | HCl leach residue | 79.5 | 14.66 | 1.91 | 0.13 | 1.81 |
| | $H_2SO_4$ leach residue | 79.9 | 14.41 | 1.88 | 0.13 | 1.83 |
| Standard slag: Oxidised in the solid state | Feed | 85.1 | 10.66 | 0.91 | 0.14 | 1.50 |
| | HCl leach residue | 87.5 | 8.27 | 0.97 | 0.09 | 1.26 |
| | $H_2SO_4$ leach residue | 86.7 | 8.84 | 0.94 | 0.12 | 1.30 |
| High iron slag: Oxidised in the solid state | Feed | 78.3 | 16.59 | 1.29 | 0.20 | 1.20 |
| | HCl leach residue | 80.1 | 15.57 | 1.32 | 0.19 | 1.32 |
| | $H_2SO_4$ leach residue | 79.4 | 15.69 | 1.30 | 0.18 | 1.22 |
| Standard slag: Oxidised in the molten state | Feed | 80.1 | 15.31 | 1.66 | 0.33 | 1.62 |
| | HCl leach residue | 79.4 | 15.69 | 1.30 | 0.18 | 1.22 |
| | $H_2SO_4$ leach residue | 79.9 | 14.15 | 1.64 | 0.26 | 1.67 |
| High iron slag: Oxidised in the molten state | Feed | 74.6 | 21.61 | 1.74 | 0.23 | 1.37 |
| | HCl leach residue | 74.3 | 20.84 | 1.75 | 0.21 | 1.48 |
| | $H_2SO_4$ leach residue | 74.4 | 20.97 | 1.75 | 0.20 | 1.42 |
| Standard slag: Oxidised and reduced in the solid state | Feed | 85.4 | 11.12 | 0.96 | 0.12 | 0.16 |
| | HCl Leach residue | 92.1 | 2.86 | 0.41 | 0.08 | 0.12 |

The results presented in Tables 13 clearly indicate that the proper pre-treatment of titania slag is critical to ensure good leachability of impurities. With no slag pre-treatment the increase in $TiO_2$ content of the slag after leaching was less than 1 %. Granulation in air oxidises the Ti(III) in the slag to Ti(IV) and the Fe(II) to Fe(III). The implications of this pretreatment process is unclear as no significant upgrading could be achieved for the high titanium slag, but the $TiO_2$ content of the high iron slag increased from 72.5 % to 79.9 %. Oxidation in the solid as well as molten states was not beneficial and very little upgrading was achieved. As a result of the poor results achieved with the granulation and oxidation pretreatment steps it was decided to evaluate an oxidation and reduction pretreatment. This pretreatment has the advantage that during oxidation Ti(III) and Fe(II) are oxidised to insoluble phases containing Ti(IV) and Fe(III). During reduction the insoluble Fe(III)-containing phases are converted to a soluble phase containing Fe(II). In addition the experiment was conducted at a high temperature and for a longer time than the previous experiments. The results in Table 13 show that this pretreatment led to a significant increase in $TiO_2$ concentration after leaching.

**Table 14.** The effect of phosphate fluxing on the leachability of impurities from titania slag

| Chemical composition (wt%) | TiO₂ | FeO | MgO | CaO | SiO₂ | P₂O₅ |
|---|---|---|---|---|---|---|
| Slag before phosphate fluxing | 87.3 | 8.49 | 0.98 | 0.11 | 1.35 | <0.1 |
| Lime | 0.04 | 0.32 | 1.05 | 62.7 | 1.35 | <0.1 |
| Ammonium phosphate | <0.01 | 0.13 | 0.02 | 0.02 | <0.01 | 63.2 |
| Slag after phosphate fluxing | 69.5 | 8.82 | 0.80 | 2.07 | 6.62 | 7.74 |
| H₃PO₄ leach residue | 82.3 | 6.51 | 0.09 | 0.13 | 7.21 | 1.51 |
| H₂SO₄ leach residue | 82.4 | 6.15 | 0.07 | 1.16 | 7.34 | 0.62 |
| HCl leach residue | 83.4 | 6.03 | 0.09 | 0.13 | 7.21 | 1.51 |

**Table 15.** The leach results presented in Table 14 normalised to a silica free basis

| Chemical composition (wt%) | TiO₂ | FeO | MgO | CaO | P₂O₅ |
|---|---|---|---|---|---|
| Slag after phosphate fluxing | 74.4 | 9.45 | 0.86 | 2.22 | 8.29 |
| H₃PO₄ leach residue | 88.7 | 7.02 | 0.10 | 0.14 | 1.62 |
| H₂SO₄ leach residue | 88.9 | 6.63 | 0.08 | 1.25 | 0.67 |
| HCl leach residue | 90.2 | 6.52 | 0.10 | 0.04 | 0.77 |

The phosphate fluxing pretreatment was attempted because the morphology of the slag is modified to rutile crystals set in a phosphate glass that contains all the impurities. The results of phosphate fluxing experiment are presented in Table 14. It shows the chemical analysis of the slag before and after the phosphate fluxing procedure and that of the leach residues after leaching in phosphoric acid, sulphuric acid and hydrochloric acid respectively. It is immediately obvious from the high silica values that contamination of the slag occurred during the slag preparation procedure. This is confirmed by the low silica contents of the different feed materials used in the preparation procedure. The leach results were normalised to a silica free basis by recalculating the chemical compositions without any silica. The adjusted values are presented in Table 15. This shows that the $TiO_2$ content of the slag increased to more than 90% after phosphate fluxing followed by leaching in hydrochloric acid.
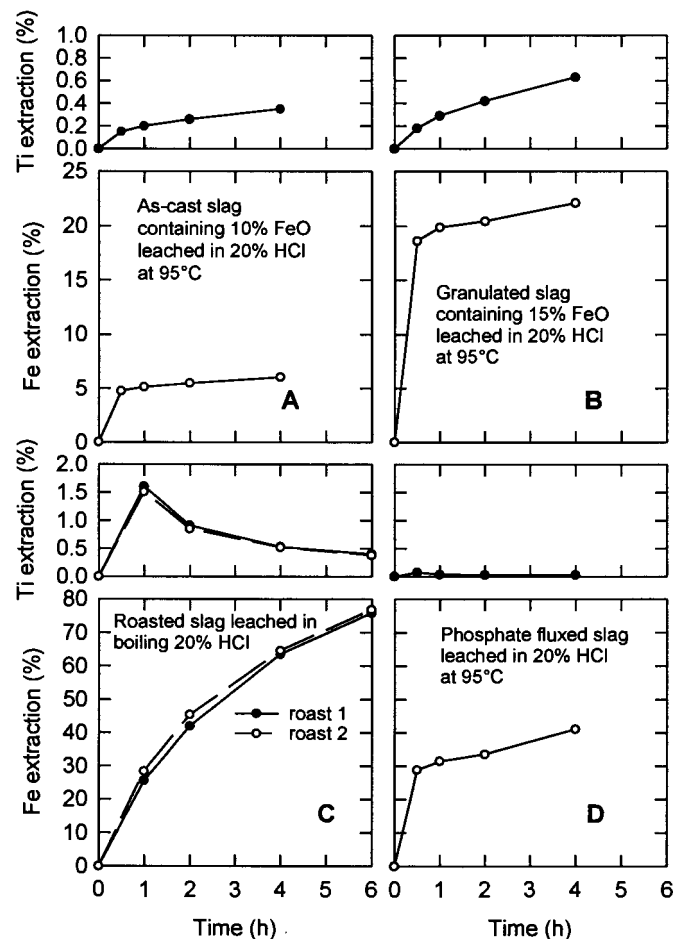
Ti extraction (%)

As-cast slag containing 10% FeO leached in 20% HCl at 95°C

Fe extraction (%)

Granulated slag containing 15% FeO leached in 20% HCl at 95°C

**A**

**B**

Ti extraction (%)

Roasted slag leached in boiling 20% HCl

roast 1
roast 2

Phosphate fluxed slag leached in 20% HCl at 95°C

Fe extraction (%)

**C**

**D**

Time (h)　　　Time (h)

**Figure 3.** The leach kinetics of titanium and iron in 20% HCl from: **A** Standard as-cast slag at 95°C; **B** High iron granulated slag containing at 95°C; **C** Oxidised and reduced slag at 107°C and; **D** Phosphate fluxed slag at 95°C

Figure 3-A shows the extraction curves for Fe and Ti from as-cast slag and it is evident that with no pre-treatment very little iron or titanium are leached. Most of the initial slag pre-treatment procedures did not enhance the leachability of the slag (Table 13). Granulation of the slag which contained 15 % FeO did however increase the leachability of the slag markedly. Figure 3-B shows that almost 25 % of the iron was leached from this slag in a hydrochloric acid solution at 95 °C. The best pre-treatment process proved to be the oxidation-reduction roast procedure; Figure 3-C shows that almost 80 % of the iron was extracted in a boiling hydrochloric acid solution. Figure 3-C also shows the titanium extraction with leaching time; it increases to more than 1.5 % in the first half an hour before it decreases to less than a half percent after four hours. This result is interesting as it is similar to the results published by Sinha (1984) for ilmenite leaching in HCl. He explained this phenomenon by noting that both iron and titanium initially go into solution but as leaching proceeds the amount of titanium in solution decreases as a result of hydrolysis and precipitation. He also described how fines are formed during this

15

reaction. Apparently factors such as agitation rate, acid concentration, temperature and ferrous chloride concentration dictate if the hydrolysis and precipitation of titanium occur in the bulk solution or in the particles. If it occurs in the bulk solution fines are formed. This occurrence of this phenomenon in the experiments is confirmed by the presence of white fines in the leach solutions of the oxidised and reduced slag. Figure 3-D shows that more than 40 % of the iron was extracted from the slag and that almost no titanium was dissolved. These results were achieved despite a high FeO value of ~ 9 % in the feed material. Oden, Summer and Howe (1973) found that high iron values were detrimental to the leachability of impurities from phosphate fluxed slag. Van Dyk (1996) achieved a high iron extraction from a slag containing ~6 % FeO. This suggests that the $TiO_2$ content can be increased even further if a slag with a low iron content is subjected to the phosphate fluxing procedure.

A mineralogical investigation was conducted on the standard as-cast slag as well as the slag oxidised in air at 850 °C for 2 h and reduced for 20 min in a 66 % CO and 33 % $CO_2$ atmosphere. The leach residue of the roasted slag was also investigated. Table 16 gives the phase compositions of the samples as determined by X-ray diffraction (XRD). The primary phase in the as-cast slag is an iron titanium solid solution ($M_3O_5$). Trace amounts of rutile could also be detected. After oxidation and reduction the main phase in the slag was rutile, while the $M_3O_5$ phase was reduced to a trace component. A trace of ilmenite was also present. Leaching did not alter the phase composition dramatically as only the ilmenite phase disappeared.

**Table 16.** Phase-chemical composition of the slag, given in order of decreasing abundance.

| Sample | Mineralogical composition | | |
|---|---|---|---|
| | Main phases | Minor phases | Trace phases |
| Standard as cast slag | FeTi-Oxide ($M_3O_5$) | - | Rutile |
| Oxidised and reduced slag | Rutile | - | Ilmenite; FeTi-Oxide ($M_3O_5$) |
| Oxdised, reduced and leached slag | Rutile | - | FeTi-Oxide ($M_3O_5$) |

Legend :Rutile - $TiO_2$; FeTi-Oxide - $M_3O_5$-solid solution and Ilmenite - $FeTiO_3$

## 2.4 Conclusions

This study showed that slag pre-treatment is vital to achieve a high extraction of iron from titania slag during leaching. The two pre-treatment processes that showed the most promise were an oxidation-reduction roast procedure and phosphate fluxing of the slag. Although high extraction of iron was obtained it was not high enough to yield a beneficiated slag product containing more than 95 % $TiO_2$.

# 3. PROCESS DEVELOPMENT PHASE 1

## 3.1 Introduction

The preliminary investigation on processes for the production of BTS indicated that a process consisting of oxidation-reduction roasting followed by atmospheric leaching in boiling hydrochloric extracted most of the impurities from the slag. The aim of this phase of the process development was to determine the optimum roasting and leaching conditions to obtain a BTS grade of >95 % $TiO_2$. The flexibility of the process with regard to feed slag composition was also investigated.

## 3.2 Experimental design

### 3.2.1 Feed material

The slag used for this investigation was obtained from the 6th IHM 3MVA plasma furnace campaign of July 1997. The complete chemical analyses of the slags are listed in Appendix III. Table 17 shows the concentration of selected species in the feed slags.

**Table 17.** Concentration of selected species in the feed slags used for this investigation.

| Sample no. | Cast no. | TiO₂ | Ti₂O₃ | Fe | FeO | Cr₂O₃ | MgO |
|---|---|---|---|---|---|---|---|
| PFE418 | K6-S-26 | 51.80 | 30.00 | - | 8.58 | 0.30 | 2.65 |
| PFE436 | K6-S-02 | 58.40 | 13.60 | - | 21.90 | 0.11 | 1.52 |
| PFE437 | K6-S-29 | 50.90 | 33.40 | - | 8.70 | 0.17 | 1.33 |
| PFE467 | K6-S-06 | 57.00 | 21.20 | 0.82 | 14.30 | 0.11 | 1.17 |
| PFE468 | K6-S-35 | 52.30 | 32.10 | 0.03 | 9.34 | 0.12 | 1.17 |
| PFE655 | K6-S-03 | 66.10 | 9.10 | 1.58 | 15.60 | 0.11 | 3.55 |
| PFE656 | K6-S-26 | 58.00 | 22.20 | 0.35 | 9.45 | 0.28 | 2.50 |
| PFE657 | K6-S-30 | 50.70 | 34.20 | 0.21 | 7.65 | 0.15 | 1.42 |
| PFE658 | K6-S-46 | 53.90 | 28.70 | 0.27 | 9.71 | 0.12 | 1.95 |

An Australian coal from Wallarah was used for the reduction experiments. The analysis for this coal is given in Table 18.

**Table 18.** Coal analysis.

| | |
|---|---|
| Total moisture | 9.0% |
| Inherent moisture | 3.5% |
| Volatile matter | 30.0% |
| Fixed carbon | 53.0% |
| Sulphur | 0.33% |
| Ash | 13.5% |
| Calorific value | 27 MJ/kg |

### 3.2.2 Experimental plan

The variables that were investigated during the roast study are listed in Table 19. The roast conditions were evaluated by conducting a 5 h atmospheric leach with boiling 20 % HCl and determining the $TiO_2$ content of the leach residue.

**Table 19.** Variables investigated during the roast study

| Variable | Conditions |
|---|---|
| Roast temperature | 750 °C; 800 °C; 850 °C; 950 °C |
| Oxidation time | 60 min; 120 min; 180 min; 240 min |
| Reduction time | 0 min; 10 min; 20 min,;40 min |

The variables that were investigated during the leach study are listed in Table 20.

**Table 20.** Variables investigated during the leach study

| Variable | Conditions |
|---|---|
| Feed slag composition | < 10 % FeO; >10 % FeO; >2 % MgO |
| Acid concentration | 18 % HCl; 20 % HCl; 33 % HCl |
| Excess Acid | 20 %; 40 %; 70 % |
| Leach time | 0 h; ½ h; 1 h; 2 h; 4 h; 6 h; 8 h; 12 h |

### 3.2.3 Experimental procedure

#### 3.2.3.1 Roast procedure

A 100 mm diameter fluidised bed roaster was used for roasting. The roaster was fitted with an externally gas fired muffle that was used for starting-up the furnace and to control the temperature inside the furnace. The fluidisation gases were passed through rotameters. Char or coal depending on the requirement was added to the roaster with a variable speed feeder. This did not allow close control over the oxygen potential in the roaster, but is does replicate the operation of an industrial roaster. During oxidation air at a rate of 1.35 $m^3$/h (STP) was used and char, produced by a previous reduction roast, was fed into the roaster at 0.4 kg/h. For reduction air at a rate of 0.14 $m^3$/h (STP) was mixed with nitrogen at a rate of 0.67 $m^3$/h (STP). Coal was fed into the roaster at a rate of 1.0 kg/h. A test was started by passing the fluidisation gas through the reactor. 5 kg slag was then added while the gas-fired muffle was used to heat the reactor. At 650°C the char feed was started. Oxidation was taken to have commenced once the reactor temperature reached a value 50 °C below the set value. The bed temperature was controlled by adjusting the gas burner and the flue damper. During oxidation the roaster ran autothermally. At the completion of the oxidation roast a sample was taken and the reduction conditions were implemented. This was accomplished by reducing the airflow, adding nitrogen and changing the char feed to coal. The reduction temperature was maintained at 50 °C below the oxidation temperature. The roaster did not operate auto thermally during reduction and the gas fired muffle had to be used to maintain the required temperature. At the end of an experiment the slag was cooled rapidly by inserting a water-cooled lance into the bed and by changing the fluidisation gas to nitrogen alone. Char and ash were removed from the slag samples by screening at 1 mm followed by panning. The wet slag was dried at 110 °C.

#### 3.2.3.2 Leach procedure

Roasted slag was leached in boiling 20 wt % hydrochloric acid for 5 to 12 h (unless otherwise specified). Conical Quickfit flasks equipped with condensers were heated on a hot plate. No stirring was provided. At the end of the leach the solution was assayed titrimetrically for Fe (II) and Fe (III). The method used for this titration is

described in the Appendix VI. The leach liquor was decanted from the leach residue before the residue was washed. Slimes were separated from the leach solution by flocculation with a commercial flocculation agent called magnafloc. The leach residue and slimes were calcined at 850 °C for 1 h before weighing. The leach residues were analysed by inductively coupled plasma optical emission spectroscopy (ICP-OES) at the ITEC Services laboratories in Pretoria. Some solution samples were analysed by ALS, an Australian laboratory.

## 3.3 Results and discussion

### 3.3.1 Roast investigation

A series of experiments were conducted on feed slag PFE437 (88% $TiO_2$) to determine the optimum roast conditions. The results of the roast investigation are summarised in Table 21. The complete chemical analyses of the samples are listed in Appendix IV.

**Table 21.** Results of the roast investigation on feed slag PFE437.

| PFE No | Roast No. | Sample No. | Oxidation Temp. (°C) | Oxidation Time (min) | Reduction Temp. (°C) | Reduction Time (min) | % TiO₂ in leach residue |
|---|---|---|---|---|---|---|---|
| 696 | 1 | 1 | 950 | 60 | 900 | 0 | 85.50 |
| 698 | | 2 | 950 | 60 | 900 | 10 | 86.60 |
| 700 | | 3 | 950 | 60 | 900 | 20 | 87.10 |
| 702 | | 4 | 950 | 60 | 900 | 40 | 87.00 |
| 704 | 2 | 5 | 950 | 120 | 900 | 0 | 85.40 |
| 706 | | 6 | 950 | 120 | 900 | 10 | 87.90 |
| 708 | | 7 | 950 | 120 | 900 | 20 | 88.00 |
| 710 | | 8 | 950 | 120 | 900 | 40 | 87.60 |
| 712 | 3 | 9 | 950 | 240 | 900 | 0 | 84.60 |
| 714 | | 10 | 950 | 240 | 900 | 10 | 87.00 |
| 716 | | 11 | 950 | 240 | 900 | 20 | 87.40 |
| 718 | | 12 | 950 | 240 | 900 | 40 | 87.30 |
| 720 | 4 | 13 | 850 | 60 | 800 | 0 | 86.80 |
| 722 | | 14 | 850 | 60 | 800 | 10 | 90.10 |
| 724 | | 15 | 850 | 60 | 800 | 20 | 90.70 |
| 726 | | 16 | 850 | 60 | 800 | 40 | 90.20 |
| 728 | 5 | 17 | 850 | 120 | 800 | 0 | 86.70 |
| 730 | | 18 | 850 | 120 | 800 | 10 | 91.10 |
| 733 | | 19 | 850 | 120 | 800 | 20 | 92.40 |
| 734 | | 20 | 850 | 120 | 800 | 40 | 91.50 |
| 736 | 6 | 21 | 850 | 240 | 800 | 0 | 85.70 |
| 738 | | 22 | 850 | 240 | 800 | 10 | 89.00 |
| 740 | | 23 | 850 | 240 | 800 | 20 | 91.00 |
| 742 | | 24 | 850 | 240 | 800 | 40 | 85.40 |
| 744 | 7 | 25 | 800 | 180 | 750 | 0 | 86.60 |
| 746 | | 26 | 800 | 180 | 750 | 10 | 89.70 |
| 748 | | 27 | 800 | 180 | 750 | 20 | 88.60 |
| 750 | | 28 | 800 | 180 | 750 | 40 | 89.40 |
| 752 | 8 | 29 | 800 | 240 | 750 | 0 | 86.70 |
| 754 | | 30 | 800 | 240 | 750 | 10 | 89.50 |
| 756 | | 31 | 800 | 240 | 750 | 20 | 89.20 |
| 758 | | 32 | 800 | 240 | 750 | 40 | 88.90 |
| 760 | 9 | 33 | 750 | 240 | 700 | 0 | 87.90 |
| 762 | | 34 | 750 | 240 | 700 | 10 | 87.40 |

The results presented in Table 21 were analysed with BDMP, a statistical computer package developed by the Department of Biomathematics, School of Medicine, University of California, as a factorial analysis. This showed that the optimum roast conditions are:

- Oxidation temperature: 850 °C
- Oxidation time: 3 h
- Reduction temperature: 800 °C
- Reduction time: 30 min

### 3.3.2 Leach investigation

The effects of leach time and feed slag composition were evaluated by roasting four different slags under the optimum conditions identified during the roast investigation. Separate leach experiments were then performed on the slags for times varying between ½ h and 12 h. Boiling 20% HCl, 70 % above the stoichiometric amount of acid required to dissolve the impurities, was used. The complete chemical analyses of the leach investigation samples are listed in Appendix V. A summary of the results is presented in Figure 4.
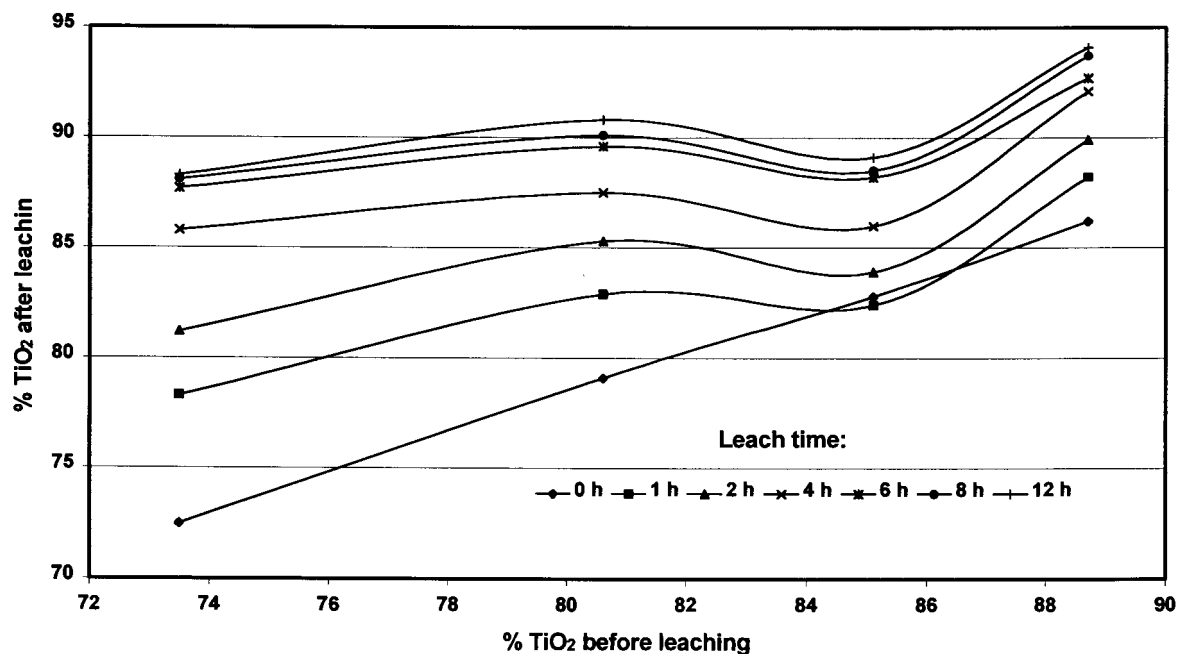


**Figure 4.** Summary of the results from the tests conducted to evaluate the effect of leach time and feed slag composition.

Figure 4 shows that slag composition influenced the BTS product quality significantly. The product with highest $TiO_2$ content was made from PFE657 (88.7 % $TiO_2$). This slag contained less than 2 % MgO and around 8 % FeO. The slag containing high levels of MgO and FeO showed up as a local minimum on the graph as they were not sufficiently upgraded (85.13 % $TiO_2$). Figure 4 also shows that long leach times are necessary to produce BTS of the required grade.

The influence of excess acid and acid concentration on the extraction of iron was investigated using PFE467 (a relatively high iron slag – see Table 12) which was oxidised for 3 h at 850 °C and reduced at 800 °C for 30 min. Three initial acid concentrations, 18%, 20% and 33% HCl were selected as these were the acid concentrations that could readily be supplied by the enhanced acid regeneration system (EARS) (Walpole, 1993) in a full scale plant. The level of excess acid was varied by keeping the solid mass constant and varying the solution volume. Solution samples were regularly taken and analysed for iron and acid. After 12 h of leaching the leach residue was analysed for $TiO_2$. The complete results are presented in the Appendix V. Figures 5 and 6 show the effect of acid concentration and level of excess acid on iron extraction. Figure 7 shows the effect of acid concentration and level of excess acid on the final product quality.
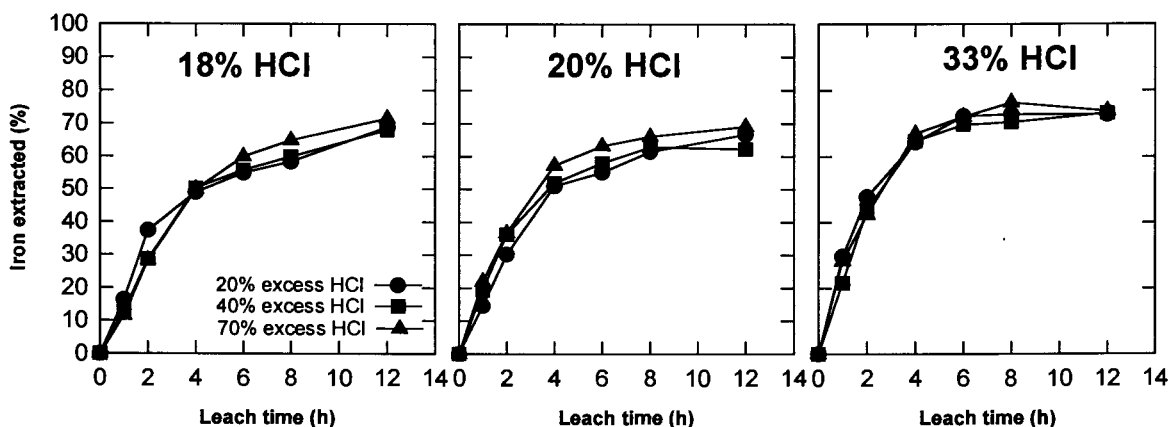


**Figure 5.** The effect of excess hydrochloric acid on iron extraction at different initial hydrochloric acid concentrations
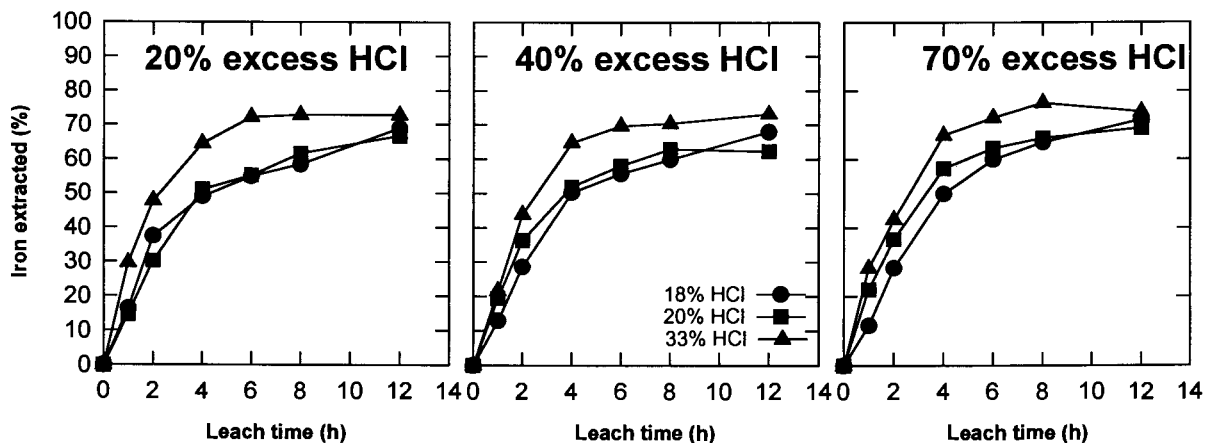


**Figure 6.** The effect of initial hydrochloric acid concentration on iron extraction at different levels of excess hydrochloric acid
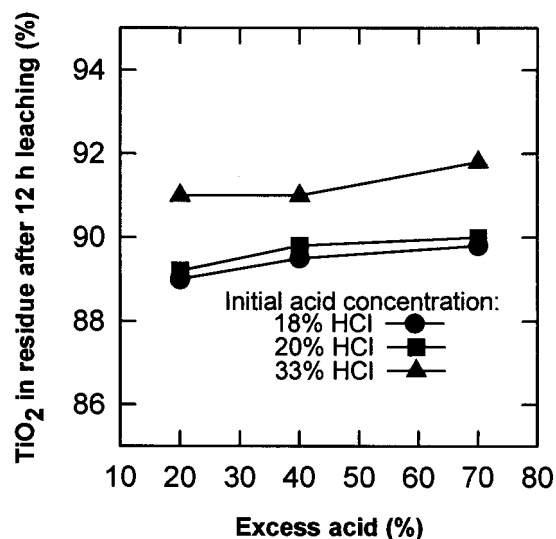
**Figure 7.** The effect of acid concentration and the level of excess acid on the final product quality after 12 h of leaching.

Figure 5 indicates that the rate of iron leaching was not significantly improved by increasing excess acid at constant initial acid concentration. On the other hand, the rate of iron leaching increased with increasing initial acid concentration at constant excess acid level (Figure 6). Final product quality improved only marginally with increasing excess acid level while it improved with increasing initial acid concentration (Figure 7). Thus, higher acid strengths improved both the kinetics of leaching and the final product quality.

### 3.3.3 Mineralogical investigation

A mineralogical investigation was conducted to determine what morphological changes occur in the slag during roasting and leaching. The investigation was conducted using three techniques: (a) X-ray diffraction analysis (XRD) (b) Optical microscopy and (c) Scanning electron microscope (SEM) analysis, using back-scattered electron imaging. The results are presented in the context of the relevant process stages of the BTS process.

3.3.3.1 As-cast titania feed slag

The phase-chemical compositions of the feed slag samples, as determined by XRD are shown in Table 22. The slag samples were all of similar mineralogical composition with the $M_3O_5$ solid solution identified as primary constituent.

**Table 22.** Phase-chemical composition of the feed slag samples as determined by XRD, given in order of decreasing abundance. The chemical compositions used to classify the slags are also given.

| PFE | Description | Chemical Composition (%) | | Mineralogical composition | | |
|-----|-------------|------|------|------------|-------|-------|
| | | FeO | MgO | Main | Minor | Trace |
| 418 | High MgO | 9.68 | 2.65 | FeTi-Oxide | - | - |
| 436 | High Iron | 24.30 | 1.52 | FeTi-Oxide | - | Ilmenite |
| 437 | Standard | 8.55 | 1.60 | FeTi-Oxide | - | Rutile |
| 467 | High Iron | 14.30 | 1.85 | FeTi-Oxide | - | - |
| 657 | Standard | 7.65 | 1.42 | FeTi-Oxide | - | - |

*Legend : FeTi-Oxide - $M_3O_5$-solid solution; Rutile - $TiO_2$; Ilmenite - $FeTiO_3$*

The standard, high iron and high MgO slag all had a similar optical appearance. The individual slag particles consisted mainly of the $M_3O_5$-solid solution. The $M_3O_5$-phase occurred as fine- to coarse-grained, angular to sub-rounded, greyish coloured particles with a smooth appearance (Figure 8). Small amounts of a silicate-rich glassy phase were visible, situated at the grain boundaries of the individual $M_3O_5$ crystals. This glass contained a second silicate-enriched glass. The silicate-rich glassy phase had a smooth appearance and contained finely disseminated metallic iron precipitates. The major glassy phase was fine crystalline with needle-like titanium oxide crystallites as well as small and large metallic iron precipitates. The larger metallic precipitates were characterised by an iron sulphide outer rim.
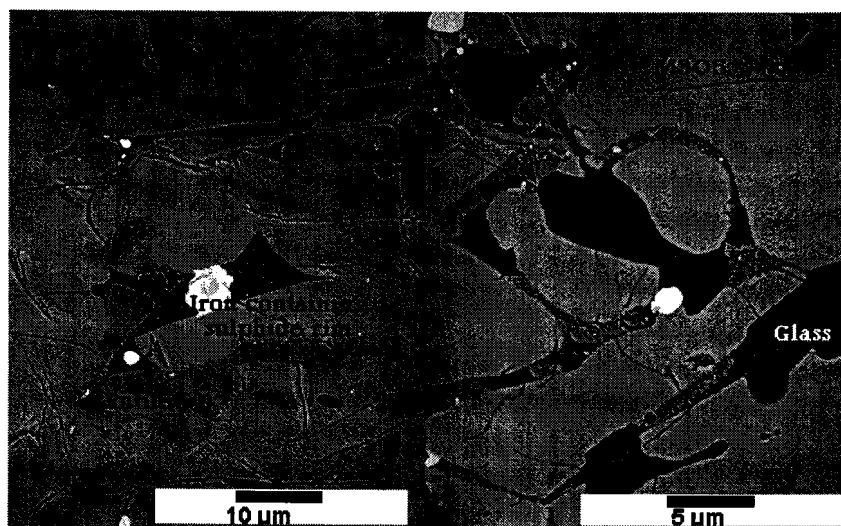


**Figure 8.** As-cast standard titania slag.

### 3.3.3.2 Oxidation

The feed slags, listed in Table 17, were all oxidised at 850 °C with exception of slag PFE437 which was oxidised respectively at 750 °C, 850 °C and 950 °C. Samples were taken after 1, 2, 3 and 4 h oxidation. The oxidised products of samples PFE437, PFE657, PFE436 and PFE418 were examined mineralogically. For the sake of the discussion they were placed in the following categories:

- Standard slag:        PFE437 and PFE657
- High iron slag:        PFE436
- High magnesia slag:    PFE418

23

*Standard slag*

The phase-chemical compositions of the individual slag samples, as obtained by XRD are shown in Tables 23 (PFE437) and 24 (PFE657). The slags consisted mainly of rutile, anatase and smaller amounts of the $M_3O_5$-solid solution after the oxidation roast. The effects of temperature and time of oxidation on the phase composition of the slag could be deduced from the data given in Tables 23 and 24. At 950 °C rutile was the main titanium dioxide-containing phase while anatase became more dominant at lower temperatures. At 850 °C both anatase and rutile occurred in more or less equal amounts and at 800 °C anatase was the main phase and rutile was present only in minor amounts. At 850 °C and reaction times of less than 1½ h, anatase appeared to be the main crystalline phase present in the samples while at longer reaction times, rutile occurred together with anatase as main crystalline phases. After a reaction period of 3 h, more rutile was present in the slag than anatase. Thus at lower temperatures the $M_3O_5$-phase transforms to anatase and a new (presumably iron-rich) $M_3O_5$-phase, while at higher temperatures the presumed new iron-rich $M_3O_5$ phase forms in conjunction with rutile. At lower temperatures the anatase transforms slowly to rutile with longer reaction times.

**Table 23.** Phase-chemical compositions of slag PFE437 after oxidation at different temperatures and times, given in order of decreasing abundance.

| PFE | Temperature (°C) | Time (h) | Mineralogical composition | | |
|---|---|---|---|---|---|
| | | | Main | Minor | Trace |
| 696 | 950 | 1 | Rutile | - | FeTi-Oxide; Anatase |
| 712 | 950 | 4 | Rutile | - | FeTi-Oxide |
| 720 | 850 | 1 | Anatase; Rutile | - | FeTi-Oxide |
| 736 | 850 | 4 | Rutile; Anatase | - | FeTi-Oxide |
| 744 | 800 | 3 | Anatase | Rutile | FeTi-Oxide |
| 752 | 800 | 4 | Anatase, | Rutile | FeTi-Oxide |
| 760 | 750 | 4 | Anatase | Rutile | FeTi-Oxide |

*Legend : FeTi-Oxide - $M_3O_5$-solid solution; Rutile - $TiO_2$; Anatase - $TiO_2$; Ilmenite - $FeTiO_3$.*

**Table 24.** Phase chemical composition of slag PFE657 after oxidation at 850 °C for different times, given in order of decreasing abundance.

| PFE | Time (h) | Mineralogical composition | | |
|---|---|---|---|---|
| | | Main | Minor | Trace |
| 924 | ½ | Anatase | Rutile; FeTi-Oxide | - |
| 925 | 1 | Anatase | Rutile | FeTi-Oxide |
| 926 | 1½ | Anatase | Rutile | FeTi-Oxide |
| 927 | 2 | Anatase; Rutile | - | FeTi-Oxide |
| 928 | 2½ | Anatase; Rutile | - | FeTi-Oxide |
| 929 | 3 | Rutile; Anatase | - | FeTi-Oxide |

*Legend : FeTi-Oxide - $M_3O_5$-solid solution; Rutile - $TiO_2$; Anatase - $TiO_2$; Ilmenite - $FeTiO_3$.*

An optical as well as a SEM investigation were conducted on polished blocks of the oxidised samples. The SEM images were generated from back scattered electrons. This allowed areas of iron concentration to be visible in micrographs of the slag as compositional differences were highlighted by a change in tone. Areas rich in iron were very light and appeared almost white.

The majority of the slag particles had a zoned appearance. In the centre of the particles was a $M_3O_5$ core surrounded by a $TiO_2$-rich mantle. Most of the iron migrated outwards to form an iron-enriched zone on the outsides of the particles. This marginal zone was slightly porous and rutile was also present (Figure 9). Iron migration towards the edges of cracks also occurred. The unreacted $M_3O_5$-cores

24

contained fine metallic iron precipitates situated at the edges of cracks that extended through the slag particles. As in the unreacted slag, small amounts of silicate-rich glass were present at the grain boundaries. This glass contained fine needle-like titania-rich crystallites as well a second silica-enriched glassy phase. Small and large metallic iron precipitates were present. The larger metallic precipitates contained iron-sulphide outer rims.
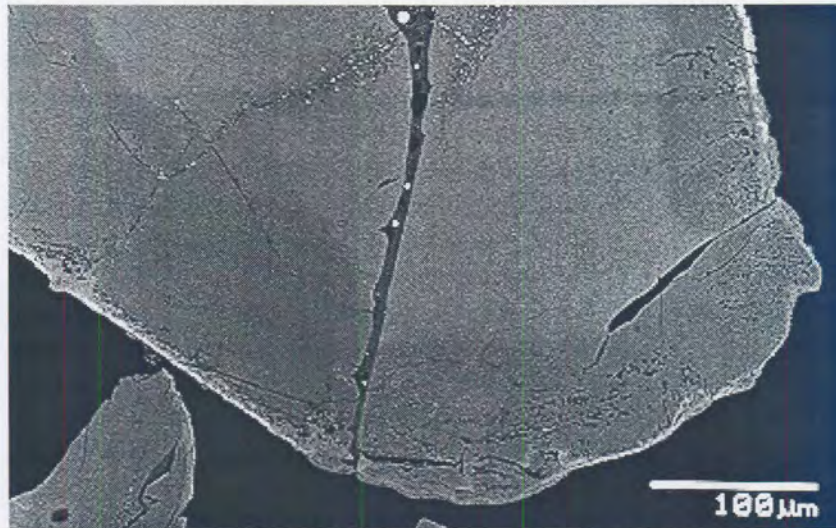


**Figure 9.** Standard slag oxidised for 1 h at 850 °C, displaying iron migration towards the edges of cracks and the outer rims of the particles.
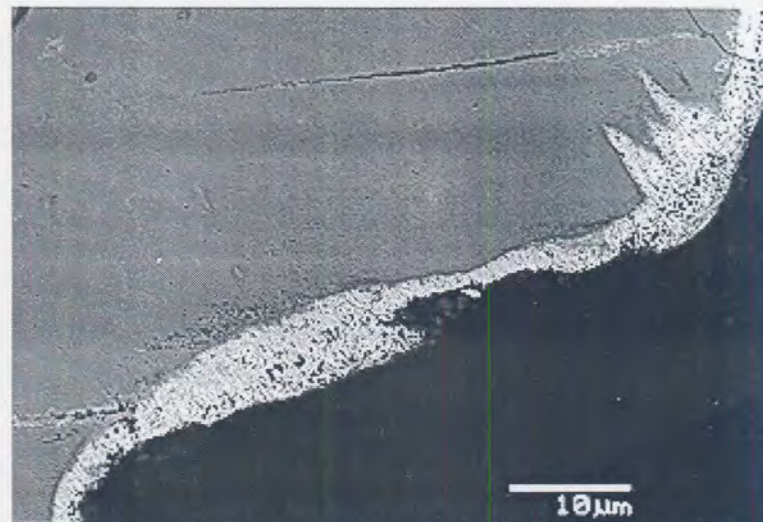


**Figure 10.** Standard slag oxidised for 3 h at 800 °C, contained dense particles that displayed iron enrichment to the outsides of the particles.

Minor differences were observed between the different oxidation samples concerning the degree of reaction and general appearance of the individual slag particles. Only the largest slag particles contained unreacted cores, in the sample roasted for 1 h at 950 °C, and these cores were smaller compared with samples roasted at lower temperatures. The smaller particles were completely oxidised. A few particles contained thin, dense rutile rims. Slag oxidised at 850 °C for respectively 1 and 4 h demonstrated the effect of longer oxidation times. Both slag samples contained coarse-grained particles with unreacted $M_3O_5$-cores surrounded by $TiO_2$-rich mantles

and porous outer rims. Particles displaying incomplete transformation were less abundant in the sample oxidised for 4 h. Slag oxidised for 3 h at 800 °C contained many particles displaying well-defined unreacted $M_3O_5$-cores. Most of the oxidised slag particles appeared to be dense and only a small portion of the particles was slightly porous. Iron migration occurred towards the outer rims of the slag particles as well as the edges of cracks extending through the particles (Figure 10). Fine metallic iron precipitates were present along the edges of these cracks.
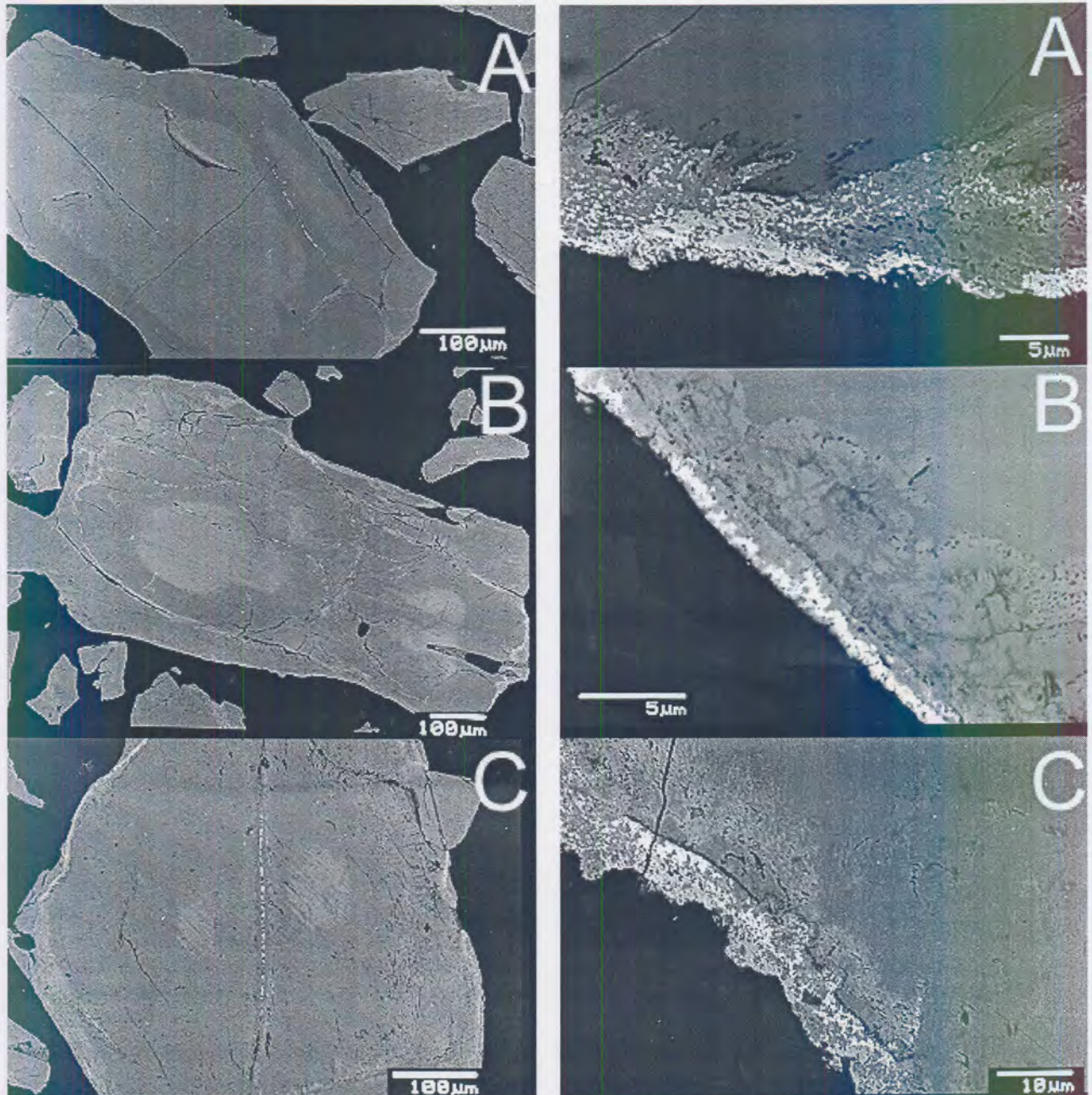


**Figure 11.** (Left side) Longer oxidation times resulted in a decrease in the size of the unreacted cores in the particles and an increase in the amount of iron migration to the outsides of the particles. (Right side) Two distinct phases were visible in the iron-enriched rim on the outsides of the oxidised particles.
**A:** *Standard slag oxidised for 1 h at 850 °C*
**B:** *Standard slag oxidised for 1½ h at 850 °C*
**C:** *Standard slag oxidised for 3 h at 850 °C*

The effect of oxidation time was evident from samples roasted at 850°C for times ranging between ½ h and 3 h (Table 24 and Figure 11). The slag samples oxidised for ½, 1 and 1½ h had a zoned appearance, with large unreacted $M_3O_5$ cores in the particles centres surrounded by thin $TiO_2$-rich mantles. The outer margins of the particles were enriched in iron. These particles were dense overall and only the outer margins were slightly porous. Longer oxidation times resulted in a decrease in the size of the unreacted cores and in an increase in the amount of iron migration to the outer margins of the slag particles (Figure 11). An interesting observation was the presence of two distinct phases in the iron-enriched zone on the outsides of the particles.

*High iron slag*

The phase-chemical compositions of the slag samples as obtained by XRD analysis, are listed in Table 25. The oxidised slag contained mainly $M_3O_5$ and anatase. Rutile was present in minor amounts. Trace amounts of ilmenite present in the as-cast feed slag (PFE436) were still present after oxidation for respectively 1, 2 and 3 h at 850 °C. With increasing oxidation time, anatase appears to convert to rutile. This is evident in the sample oxidised for three hours (PFE769) where rutile is present as a main component.

**Table 25.** Phase-chemical composition of the high iron containing slag PFE436 after oxidation at 850 °C with increasing time, given in order of decreasing abundance.

| PFE | Time | Mineralogical composition | | |
|---|---|---|---|---|
| | (h) | Main | Minor | Trace |
| 765 | 1 | FeTi-Oxide/Anatase | Rutile | Ilmenite |
| 767 | 2 | FeTi-Oxide/Anatase | Rutile | Ilmenite |
| 769 | 3 | FeTi-Oxide/Anatase; Rutile | - | Ilmenite |

*Legend : FeTi-Oxide - $M_3O_5$-solid solution; Rutile - $TiO_2$; Anatase - $TiO_2$; Ilmenite - $FeTiO_3$.*

The optical and SEM analysis revealed similar features in the high iron slag compared to the standard slag. The most significant feature was the iron migration towards the outer margins of the individual slag particles as well as the edges of cracks (Figure 12). This feature was clearly recognised in all the samples. The sample oxidised for 1 h contained a number of the slag particles with large unreacted $M_3O_5$-cores and relatively "thin" $TiO_2$-rich mantles. Longer oxidation times resulted in a more complete conversion of the slag to rutile/anatase (Figure 13). After 3 h oxidation the size of the unreacted cores had diminished resulting in broader $TiO_2$-rich mantles. The finer-grained particles were completely oxidised and transformed to rutile/anatase. The effects of oxidation were also visible along cracks extending through the slag particles, as rutile and finely disseminated metallic iron precipitates were visible adjacent to cracks in the unreacted $M_3O_5$ cores. With longer oxidation times the metallic iron appeared more abundant in the cracks. During oxidation the transformed mantles became slightly porous, while the unreacted cores remained dense.
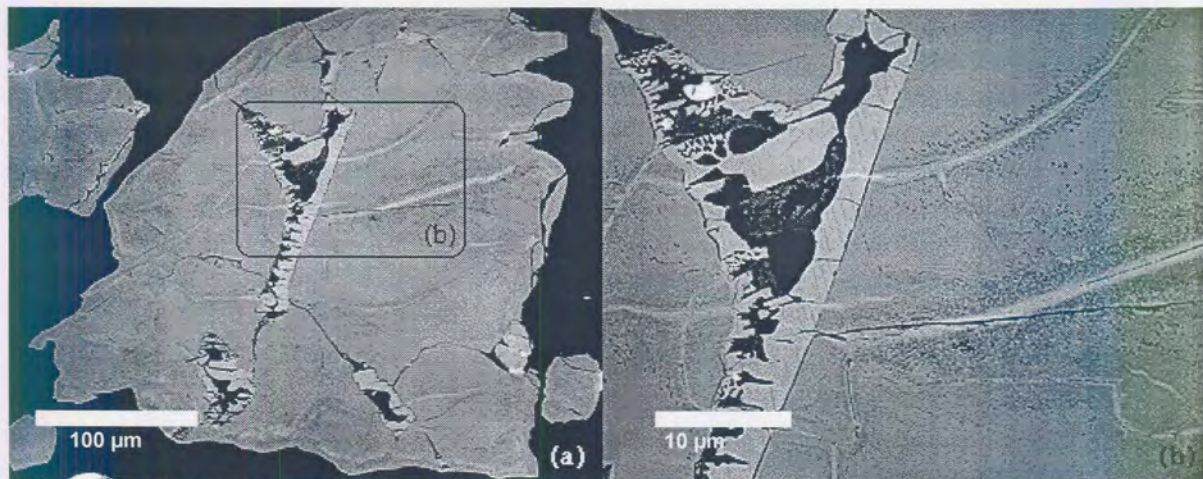
**Figure 12**. High iron slag particle oxidised for 1 h at 850 °C displaying iron migration towards the edges of cracks leaving the adjacent areas enriched in titania and slightly porous. Particle core consisted of the $M_3O_5$-solid solution. The glass phase depicted in micrograph (b) contained ilmenite.
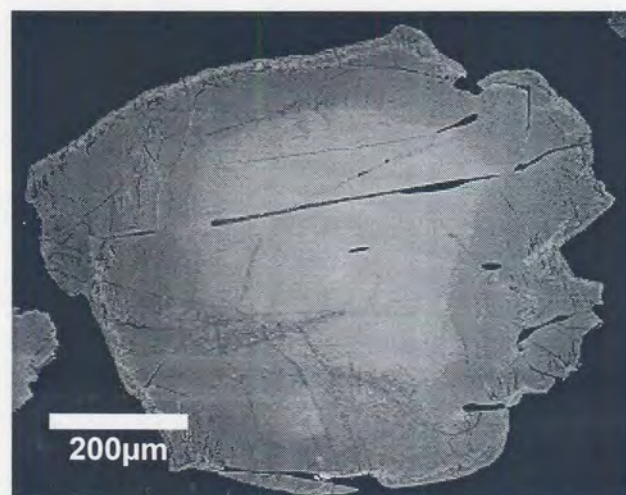


**Figure 13**. High iron slag particle oxidised at 850 °C for 3 h displaying a well defined zoned texture with $M_3O_5$-rich inner core, $TiO_2$-rich mantle and porous, iron-enriched outer rim.

High magnesia slag

The phase-chemical compositions of the slag samples as obtained by XRD analysis, are listed in Table 26. This shows that the $M_3O_5$-solid solution, anatase and rutile were present as main crystalline phases in the slag oxidised for 1 h at 850 °C. After 2 h of oxidation the amount of rutile increased to such an extent that the $M_3O_5$ and anatase phases were reduced to minor phases. Trace amounts of ilmenite were present in this sample. This might be an intermediate product that formed during oxidation and it may be consumed with further oxidation. In the sample oxidised for three hours the amount of $M_3O_5$ decreased to below that of anatase, while rutile was still present as the main phase.

28

**Table 26.** Phase-chemical composition of the high magnesium slag PFE418 after oxidation at 850 °C with increasing time, given in order of decreasing abundance.

| PFE | Time | Mineralogical composition | | |
|-----|------|---------------------------|---|---|
| | (h) | Main | Minor | Trace |
| 771 | 1 | FeTi-Oxide/Anatase; Rutile | - | - |
| 773 | 2 | Rutile | FeTi-Oxide/Anatase | Ilmenite |
| 775 | 3 | Rutile | Anatase/FeTi-Oxide | - |

*Legend* : FeTi-Oxide - $M_3O_5$-solid solution; Rutile - $TiO_2$; Anatase - $TiO_2$; Ilmenite - $FeTiO_3$.

The optical and SEM analysis showed that the characteristic features of the high magnesium slag were similar to those of the standard slag. Most notably, iron migration also occurred towards the particle rims, but the amount of migration seemed less than that observed for the other slag compositions.

After 1 h oxidation the majority of the particles, including the finer-grained particles, contained relatively large unreacted $M_3O_5$-cores with only thin $TiO_2$-rich mantles. After 2 h oxidation the slag particles contained slightly smaller unreacted $M_3O_5$-cores and broader $TiO_2$-rich mantles. A large percentage of the finer-grained slag particles were completely oxidised, consisting mainly of rutile/anatase. After 3 h oxidation, unreacted $M_3O_5$-cores were evident only in the coarser-grained slag particles. All three oxidised slag samples contained some fine metallic iron precipitates along cracks extending through the slag particles (Figures 14 and 15). These precipitates were associated with rutile.
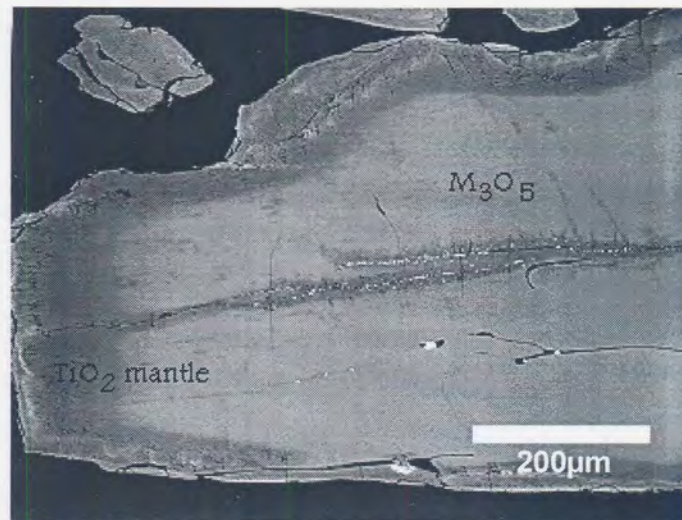


**Figure 14.** High magnesium slag (PFE418) particle oxidised for 1 h at 850 °C displaying $M_3O_5$-rich core and $TiO_2$-rich mantle with iron enrichment towards the edges of cracks and outer rim of the slag particle. Metallic iron precipitates were evident in the vicinity of internal cracks.
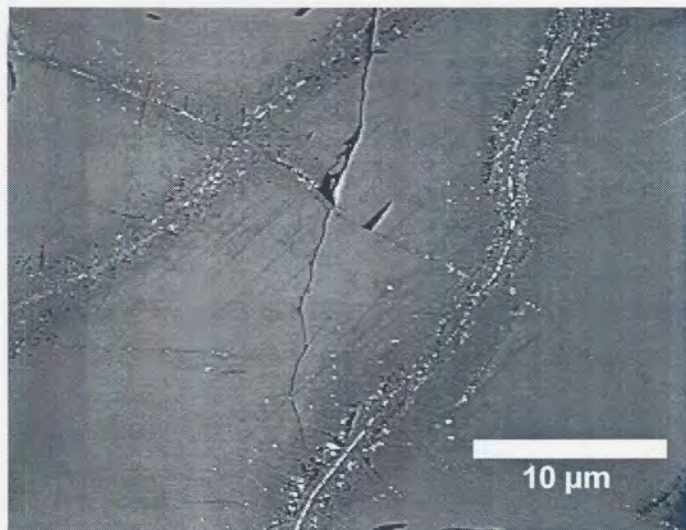
29

**Figure 15**. High magnesium slag (PFE418) particle oxidised for 1 h at 850 °C displaying $M_3O_5$-rich core with metallic iron precipitates associated with rutile along internal cracks extending through the particle.

3.3.3.3 Reduction

The different as-cast slags, which had been oxidised for respectively 1, 2, 3 and 4 h, were subjected to a reducing roast at 800°C. Samples, large enough for a leach test as well as mineralogical investigation, were taken at respectively 10, 20, 30 and 40 min.

*Standard slag*

The phase-chemical compositions of the individual reduced slag samples from the oxidised feed slag PFE437, as determined by XRD are shown in Table 27. The reduced slag samples consisted mainly of rutile and anatase with trace amounts of the $M_3O_5$-solid solution and ilmenite. When these results are compared with those presented in Table 23 for the oxidised samples it appears that no dramatic changes in the mineralogical composition of the samples occurred during the reduction process. The only noticeable difference is the presence of trace quantities of ilmenite in all of the reduced slag samples.

The reduced slag samples appeared very similar to the oxidised samples. The larger particles had unreacted $M_3O_5$ cores surrounded by reacted mantles of $TiO_2$. Iron-enriched rims were present on the outsides of the particles. The smaller particles were completely reacted and did not contain $M_3O_5$ cores. A significant difference between the oxidised samples and the reduced samples is that the iron-enriched rims converted to ilmenite in the reduced samples. The ilmenite was not visible during the optical analysis, but its presence was confirmed with EDS analysis based on the Ti/Fe ratio in the iron-enriched areas. Differences in the general appearance between slag particles that had been reduced at different temperatures for different time intervals were noticed. Particles containing unreacted cores were less abundant in the slag samples that had been reduced for respectively 20 and 40 min in comparison to those reduced for only 10 min.

**Table 27.** Phase-chemical composition of standard slag (PFE437) which had been oxidised and reduced at different temperatures and times, given in order of decreasing abundance.

| PFE | Roast conditions | | Mineralogical composition | | |
|---|---|---|---|---|---|
| | | | Main | Minor | Trace |
| 698 | 1h 950°C | 10 min | Rutile | - | FeTi-Oxide; Ilmenite; Anatase |
| 700 | Ox. (PFE696); | 20 min | Rutile | - | FeTi-Oxide; Ilmenite |
| 702 | 900°C red. for: | 40 min | Rutile | - | FeTi-Oxide; Ilmenite |
| 722 | 1h 850°C | 10 min | Anatase; Rutile | - | FeTi-Oxide |
| 724 | Ox. (PFE720); | 20 min | Anatase; Rutile | - | Ilmenite; FeTi-Oxide |
| 726 | 800°C red. for: | 40 min | Rutile; Anatase | - | Ilmenite; FeTi-Oxide |
| 738 | 4h 850°C | 10 min | Rutile; Anatase | - | FeTi-Oxide; Ilmenite |
| 740 | Ox. (PFE736); | 20 min | Rutile; Anatase | - | FeTi-Oxide; Ilmenite |
| 742 | 800°C red. for: | 40 min | Rutile; Anatase | - | FeTi-Oxide |
| 746 | 3h 800°C | 10 min | Anatase | Rutile | FeTi-Oxide; Ilmenite |
| 748 | Ox.(PFE744); | 20 min | Anatase | Rutile | FeTi-Oxide; Ilmenite |
| 750 | 750°C red. for: | 40 min | Anatase | Rutile | Ilmenite; FeTi-Oxide |
| 827 | 3h 850°C Ox. (PFE929); 800°C red. for: | 30 min | Anatase; Rutile | - | Ilmenite; FeTi-Oxide |

**Legend:** *Anatase - $TiO_2$; Rutile - $TiO_2$; FeTi-Oxide - $M_3O_5$-solid solution; Ilmenite - $FeTiO_3$*

The samples which had been oxidised at 950 °C, appeared almost completely reacted as very few particles containing unreacted $M_3O_5$-cores were present after reduction intervals of 10, 20 and 40 min. Some of the particles contained thin outer rims of densely packed rutile crystallites. Iron migration towards the edges of cracks as well as outer margins of the particles was noticeable.
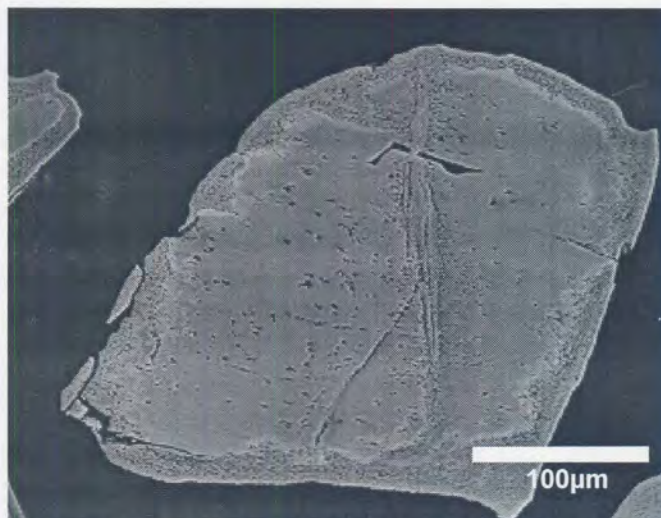


**Figure 16.** Standard slag (PFE437) particle, which had been oxidised at 850 °C for 1 h and reduced for 40 min at 800 °C displaying porosity and iron migration towards the outer margins of the particle. This particular slag particle had no unreacted core.

The slag oxidised for 1 h at 850 °C and reduced for respectively 10, 20 and 40 min at 800 °C, contained particles with unreacted cores and $TiO_2$-rich mantles. Cracks extending through the unreacted cores were characterised by the presence of rutile and fine metallic iron precipitates. The metal appeared to be more abundant in the cracks in the sample reduced for 40 min. The slag particles varied from slightly porous to dense. The reacted marginal zones were generally more porous (Figure 16). The samples which were oxidised for 4 h at 850 °C and reduced at 800 °C for

31

10, 20 and 40 min, looked very similar to the samples oxidised for 1 h but there were fewer unreacted $M_3O_5$ cores present.

The slag samples oxidised at 800 °C for 3 h and reduced at 750°C for respectively 10, 20 and 40 min, contained a large number of particles with unreacted cores and thin $TiO_2$-rich mantles. The outer margins were slightly porous and the remainder of the particles appeared to be dense. Metallic iron precipitates, associated with rutile, were present along cracks extending through the unreacted cores.

The slag sample oxidised at 850°C for 3 h and reduced at 800°C for 30 min (PFE827) contained dense unreacted $M_3O_5$ cores in only a few larger particles. The rest of the particles were fully reacted. Precipitated carbon associated with the finer-grained slag particles was present in this sample.

*High iron slag*

The phase-chemical results, as obtained by XRD, for the high iron slag subjected to oxidation and reduction, are presented in Table 28. This shows that ilmenite formed during the reduction roast. The amount of ilmenite that formed is significantly more than that formed during reduction of the standard slag. Ilmenite was present as a minor phase in the reduced high iron slag and it occurred in trace quantities in the reduced standard slag.

**Table 28.** Phase-chemical composition of the high iron slag (PFE436) which had been oxidised at 850 °C for 3 h and reduced at 800 °C for 30 min; given in order of decreasing abundance.

| PFE | Oxidised slag | Mineralogical composition | | |
|-----|---------------|------|-------|-------|
| | | Main | Minor | Trace |
| 833 | PFE769 | Anatase; Rutile | Ilmenite | FeTi-Oxide |

**Legend**: *Anatase - $TiO_2$; Rutile - $TiO_2$; FeTi-Oxide - $M_3O_5$-solid solution; Ilmenite - $FeTiO_3$*

The sample had a zoned appearance. The centre of the particles consisted of the $M_3O_5$ phase surrounded by a $TiO_2$ mantle. A iron enriched layer was present on the outer margins of the particles. The iron in the iron-rich layer was present as ilmenite. The iron-rich layers appeared wider than those observed in the standard slag (Figures 17 and 18). The sample contained large quantities of glass at the grain and crystal boundaries of the original $M_3O_5$-crystals. The outer margins of the slag particles were porous with the core-areas, slightly denser. A few of the slag particles contained thin, dense rutile-rich outer rims. Some of the slag particles displayed fine, metallic iron precipitates associated with rutile along cracks extending through the slag particles. A few of the smaller particles had graphite borders.
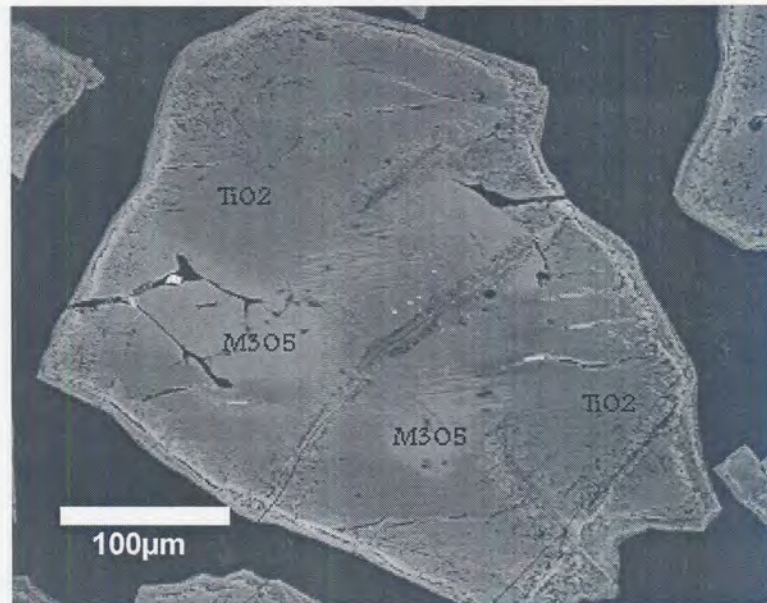
**Figure 17.** High iron slag oxidised at 850°C for 3 h and reduced at 800°C for 30 minutes containing small unreacted $M_3O_5$ cores and broad $TiO_2$ mantles. Iron enrichment towards the outer margins of the particles can be observed.
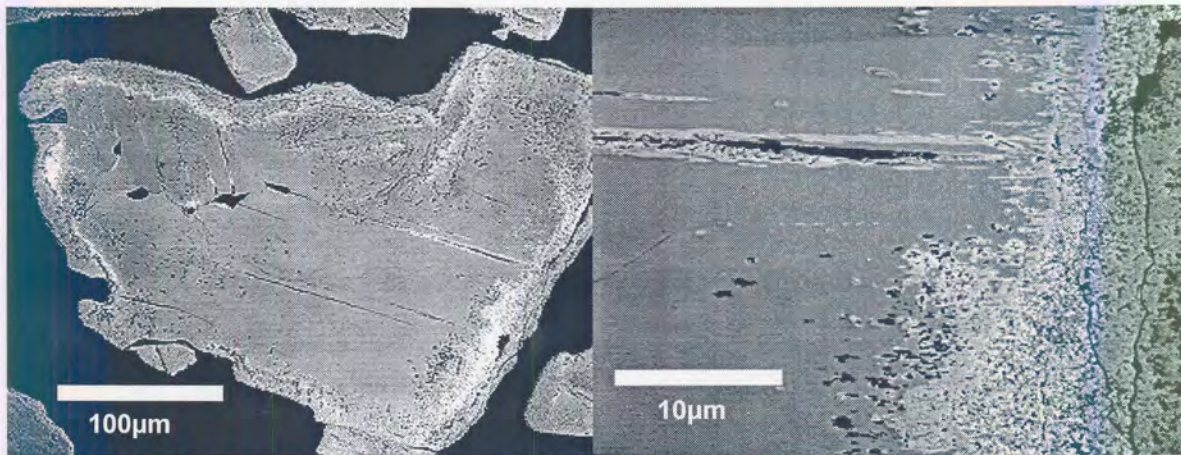
**Figure 18.** Oxidised and reduced high iron slag particle displaying iron enrichment towards the particle rim and along the edges of cracks extending through the particle.

*High magnesia slag*

The phase-chemical composition of oxidised and reduced high magnesia slag, as determined by XRD, is shown in Table 29. The main phases were rutile and anatase. The $M_3O_5$ phase was present in trace quantities along with the ilmenite that formed during reduction.

**Table 29.** Phase-chemical composition of the high magnesia slag (PFE418) which had been oxidised at 850 °C for 3 h and reduced at 800 °C for 30 min; given in order of decreasing abundance.

| PFE | Oxidised slag | Mineralogical composition | | |
|---|---|---|---|---|
| | | Main | Minor | Trace |
| 830 | PFE775 | Rutile; Anatase | | Ilmenite; FeTi-Oxide |

**Legend:** Anatase - $TiO_2$; Rutile - $TiO_2$; FeTi-Oxide - $M_3O_5$-solid solution; Ilmenite - $FeTiO_3$

The SEM investigation revealed the presence of ilmenite on the rims of the particles. The metallic iron-rutile association was still present in the few unreacted cores. Precipitated carbon was present as a thin fragile rim around some of the smaller particles (Figure 19).
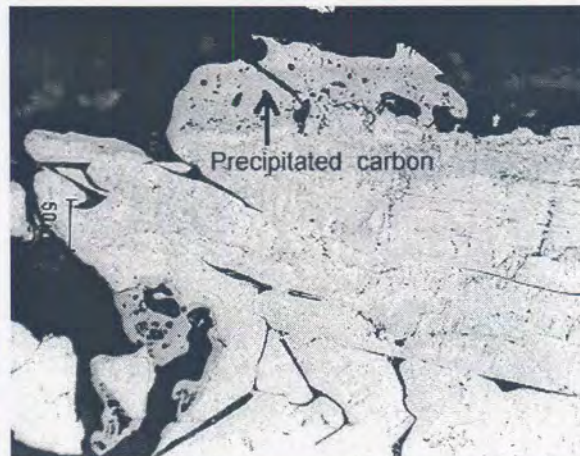


**Figure 19.** Optical micrograph of high magnesia slag which had been oxidised at 850 °C for 2 h and reduced at 800 °C for 30 min. Precipitated carbon associated with the particle is clearly visible.

3.3.3.4 Leaching

All the reduced samples were subjected to leaching in boiling 20% HCl. After 5 h of leaching the solids and liquids were separated. The solids were then calcined at 800°C for 2 h.

*Standard slag*

The phase-chemical compositions of the leach residues after calcination, as determined by XRD, are shown in Table 30. The phase compositions of the leach residues were similar to that of the oxidised products presented in Table 23. This means that the ilmenite phase that formed during reduction is removed during leaching.

Macroscopically the leached residues displayed a brownish to yellowish tint, compared to the dull black appearance of the reduced slag samples. Optically, the leached residues had a severely "weathered" appearance compared to the oxidised as well as the reduced products. Several zones could be recognised in the particles (Figure 20). The centres of the larger particles consisted of unreacted $M_3O_5$. This was surrounded by a $TiO_2$ layer that had a bluish appearance which is characteristic of anatase. The outer margins of the particles were affected by leaching and were very porous. This area had an amber appearance which is characteristic of rutile. The iron-enriched rims that were observed in the oxidised and reduced particles were almost completely removed in the leach residues. Small differences in microscopic appearance of the various leach residues were noticed. The slag reduced for 20 to 40 min appeared to be more completely leached compared to the slag samples reduced for 10 min. These particles displayed a more distinct "weathered" appearance with much broader leach affected rims. Leaching also occurred along cracks extending through the particles. Slag particles with unreacted $M_3O_5$-cores

were mainly present in the samples reduced for 10 min. The glass phase in all the samples appeared to be unaffected by leaching.

**Table 30.** Phase-chemical composition of standard slag that had been oxidised and reduced at different temperatures and times, leached for 5 h and calcined at 800 °C for 2 h, given in order of decreasing abundance.

| PFE | Roast conditions | | Final $TiO_2$ content (%) | Mineralogical composition | | |
|---|---|---|---|---|---|---|
| | | | | Main | Minor | Trace |
| 697 | Ox: 1h at 950°C | 0 min | 85.50 | Rutile | | FeTi-Oxide; Anatase |
| 699 | Red: at 900°C | 10 min | 86.60 | Rutile | | FeTi-Oxide |
| 701 | for: | 20 min | 87.10 | Rutile | | FeTi-Oxide; Anatase |
| 703 | | 40 min | 87.00 | Rutile | | FeTi-Oxide |
| 721 | Ox: 1h at 850°C | 0 min | 86.80 | Anatase; Rutile | | FeTi-Oxide |
| 723 | Red: at 800°C | 10 min | 90.10 | Anatase; Rutile | | FeTi-Oxide |
| 725 | for: | 20 min | 90.70 | Anatase; Rutile | | FeTi-Oxide |
| 727 | | 40 min | 90.20 | Rutile; Anatase | | FeTi-Oxide |
| 737 | Ox: 4h at 850°C | 0 min | 85.70 | Rutile; Anatase | | FeTi-Oxide |
| 739 | Red: at 800°C | 10 min | 89.00 | Rutile; Anatase | | FeTi-Oxide; Ilmenite |
| 741 | for: | 20 min | 91.00 | Rutile; Anatase | | FeTi-Oxide |
| 743 | | 40 min | 85.40 | Rutile; Anatase | | FeTi-Oxide |
| 751 | Ox: 4h at 800°C Red: at 750°C for: | 40 min | 89.40 | Anatase; Rutile | | FeTi-Oxide |

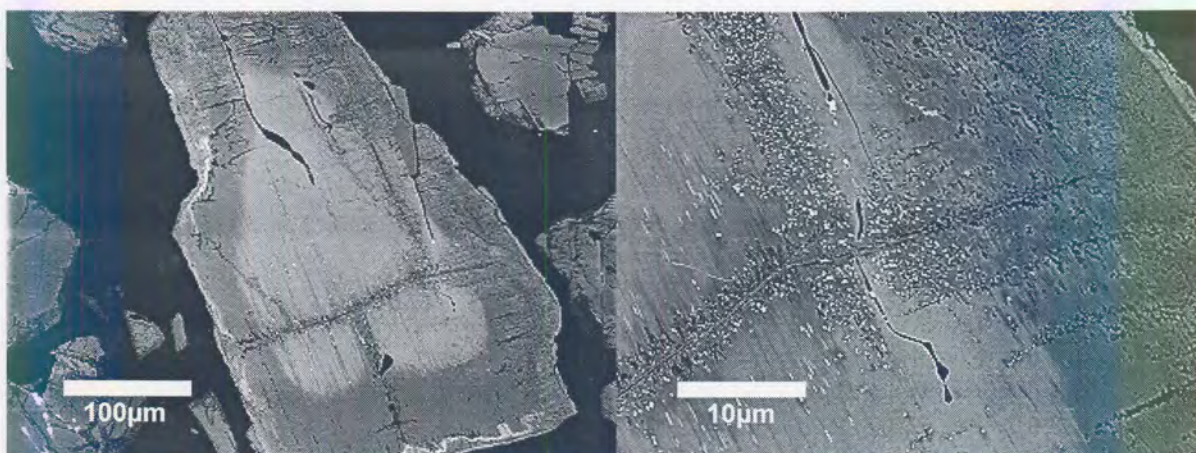*Legend: Anatase - $TiO_2$; Rutile - $TiO_2$; FeTi-Oxide - $M_3O_5$-solid solution; Ilmenite - $FeTiO_3$*



**Figure 20.** Standard slag, oxidised for 1 h at 850 °C; reduced at 800 °C for 40 min; leached for 5 h and calcined at 800°C for 2 h.

*High iron slag*

The phase-chemical composition, as determined by XRD analysis, of the high iron slag (PFE436) after it had been oxidised at 850 °C for 3 h, reduced at 800 °C for 30 min, leached for times varying between 1 and 12 h and calcined are given in Table 31. This shows that the ilmenite phase decreased from a minor phase to a phase present in trace quantities after 1 h of leaching. No ilmenite was detected after 4 h of leaching and the anatase decreased from a major phase to a minor phase. Additional leaching up to 12 h did not change the phase composition of the slag, but the $TiO_2$ content increased.

**Table 31.** Phase-chemical composition of high iron slag which had been oxidised at 850 °C for 3 h and reduced at 800 °C for 30 min, leached for different times and calcined; given in order of decreasing abundance.

| PFE | Time (h) | Final TiO$_2$ content (%) | Mineralogical composition | | |
|---|---|---|---|---|---|
| | | | Main | Minor | Trace |
| 789 | 1 | 78.30 | Rutile; Anatase | FeTi-Oxide | Ilmenite |
| 791 | 4 | 85.80 | Rutile | Anatase | FeTi-Oxide |
| 794 | 12 | 88.30 | Rutile | Anatase | FeTi-Oxide |

*Legend: Anatase - TiO$_2$; Rutile - TiO$_2$; FeTi-Oxide - M$_3$O$_5$-solid solution; Ilmenite - FeTiO$_3$*

These samples looked optically very similar to the leach residues of the standard slag. The centres of the particles were very dense and consisted primarily of anatase, while the rims of the particles, as a result of the leach procedure, were very porous. The areas affected by leaching consisted mainly of rutile. The sample which was leached for 12 h (Figure 21), was much more severely affected compared to sample which was leached for only 1 h. Leaching was especially effective at the outer rims of the slag particles as well as along cracks extending through the particles. The characteristic optical appearance of the leach residues can be seen in Figure 22. The interior of the particles appeared bluish, while the areas severely affected by leaching had an amber appearance. The predominance of rutile along the outsides of the particles might have been due to the calcination treatment. The finer-grained particles were more completely leached and appeared more porous than the coarser-grained particles. The unreacted M$_3$O$_5$ cores that were present in the particles before leaching were still present after leaching. The most significant observation from the SEM analysis was that the ilmenite rims, observed in the reduced slag, were not visible in any of the leach residues. The ilmenite that was present in the glass phase also appeared to have been leached.
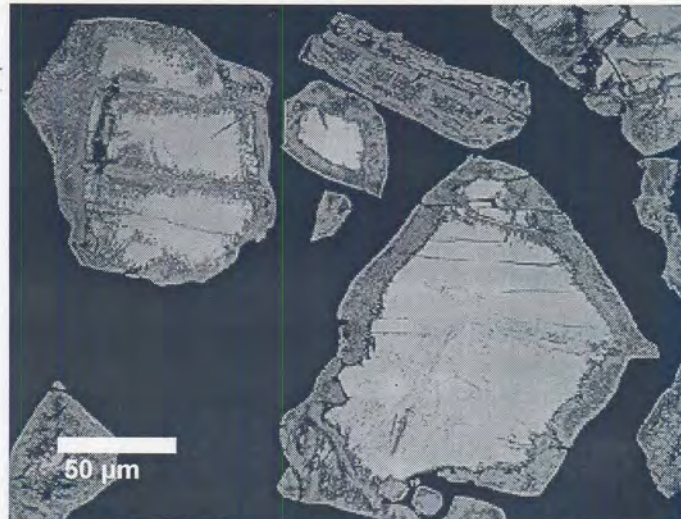


**Figure 21.** High iron slag that was oxidised, reduced and then leached for 12 h.
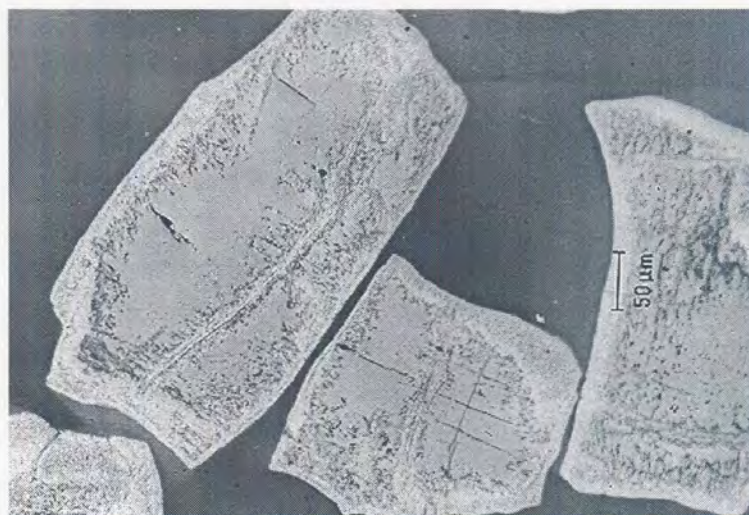
**Figure 22.** Optical micrograph of the high iron slag which was oxidised for 2 h at 850 °C, reduced for 30 min. at 800 °C, leached for 12 h and calcined. The exterior of the particles consisted predominantly of rutile and the interior predominantly of anatase.

*High magnesia slag*

The phase-chemical compositions of the leach residues from the high magnesia slag (PFE418), as obtained by XRD, are presented in Table 32. This shows that the leach residues consisted mainly of rutile. Anatase was present as a minor phase and the $M_3O_5$ phase occurred in trace amounts. No change in the phase composition of the slag was noticed with increasing leach times. A comparison between the phase compositions of the leach residues and the reduced slag reveals that the ilmenite phase is removed during leaching. Anatase also declined from a major phase to a minor phase. This may have occurred as a result of calcination; before calcination the particles appeared greyish, but after calcination all the particles had a whitish-brown appearance.

**Table 32.** Phase-chemical composition of high magnesia slag which had been oxidised at 850 °C for 3 h and reduced at 800 °C for 30 min, leached for different times and calcined; given in order of decreasing abundance.

| PFE | Time (h) | Final TiO$_2$ content (%) | Mineralogical composition | | |
| --- | --- | --- | --- | --- | --- |
| | | | Main | Minor | Trace |
| 796 | 1 | 82.40 | Rutile | Anatase | FeTi-Oxide |
| 798 | 4 | 86.00 | Rutile | Anatase | FeTi-Oxide |
| 801 | 12 | 89.10 | Rutile | Anatase | FeTi-Oxide |

*Legend: Anatase - TiO$_2$; Rutile - TiO$_2$; FeTi-Oxide - M$_3$O$_5$-solid solution; Ilmenite - FeTiO$_3$*

The individual slag particles of the high magnesia slag (Figure 23), oxidised for 3 h at 850 °C, reduced at 800 °C for 30 minutes, leached for 1 h and calcined, appeared very dense and only a very thin rim on the outside of the particles was affected by leaching. Some of the particles contained unreacted $M_3O_5$ cores. Fine metallic iron precipitates associated with rutile, could still be recognised situated along cracks extending through the unreacted cores. After 12 h of leaching the slag particles appeared more "weathered" and the affected outer margins were broader (Figure 24). The SEM analysis confirmed that, similarly to the standard and high iron slag, the iron-enriched layer on the outsides of the particles had been removed during

37

leaching. It also showed that the effect of leaching was much less severe on the high magnesia slag than on the standard slag and the high iron slag.
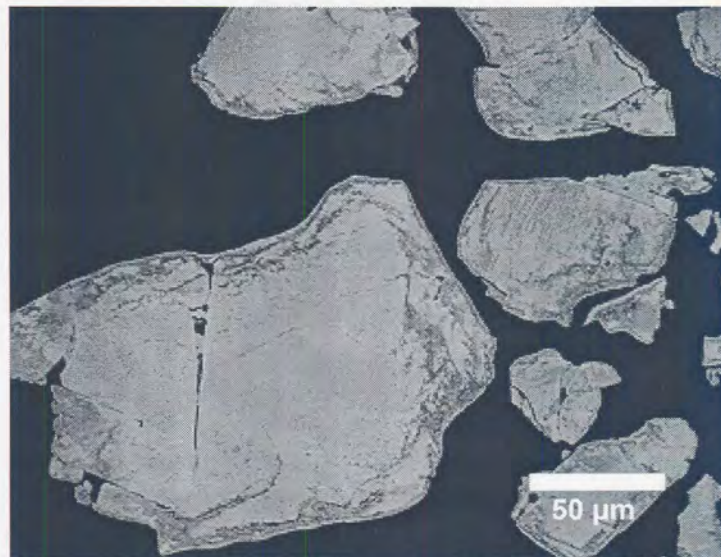


**Figure 23.** High magnesia slag, leached for 1 h; the effect of leaching is visible mainly at the outer margins of the individual slag particles.
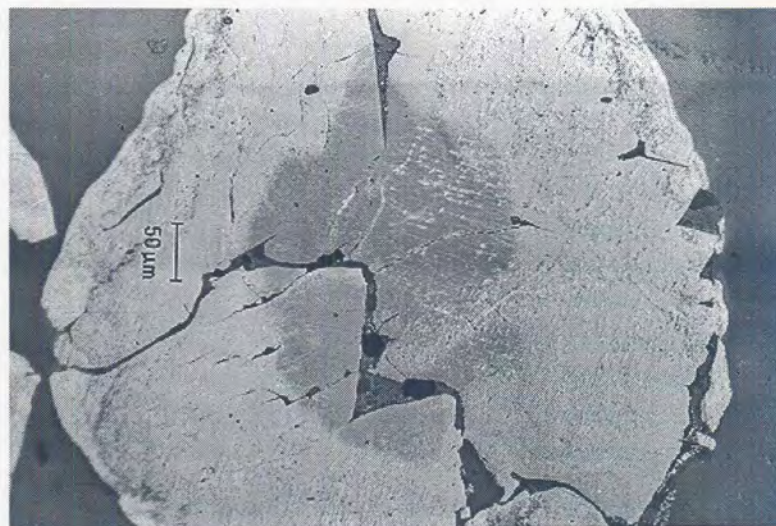


**Figure 24.** Optical micrograph of the high magnesia slag, which was oxidised for 2 h at 850 °C, reduced for 30 min. at 800 °C, leached for 12 h and calcined. The particle display a zoned appearance, in the center is an unreacted core surrounded by a mantle of anatase, while the rims consist of rutile.

### 3.3.4 Summary of the mineralogical changes that occur during roasting

3.3.4.1 Standard slag

A standard slag by definition contains about 10 % FeO and about 85 % $TiO_2$. In the **as-cast** form the slag consist mainly of the $M_3O_5$ solid solution phase (Figure 25). During **oxidation** the $M_3O_5$ phase converted to anatase, rutile and a new iron rich $M_3O_5$ phase.
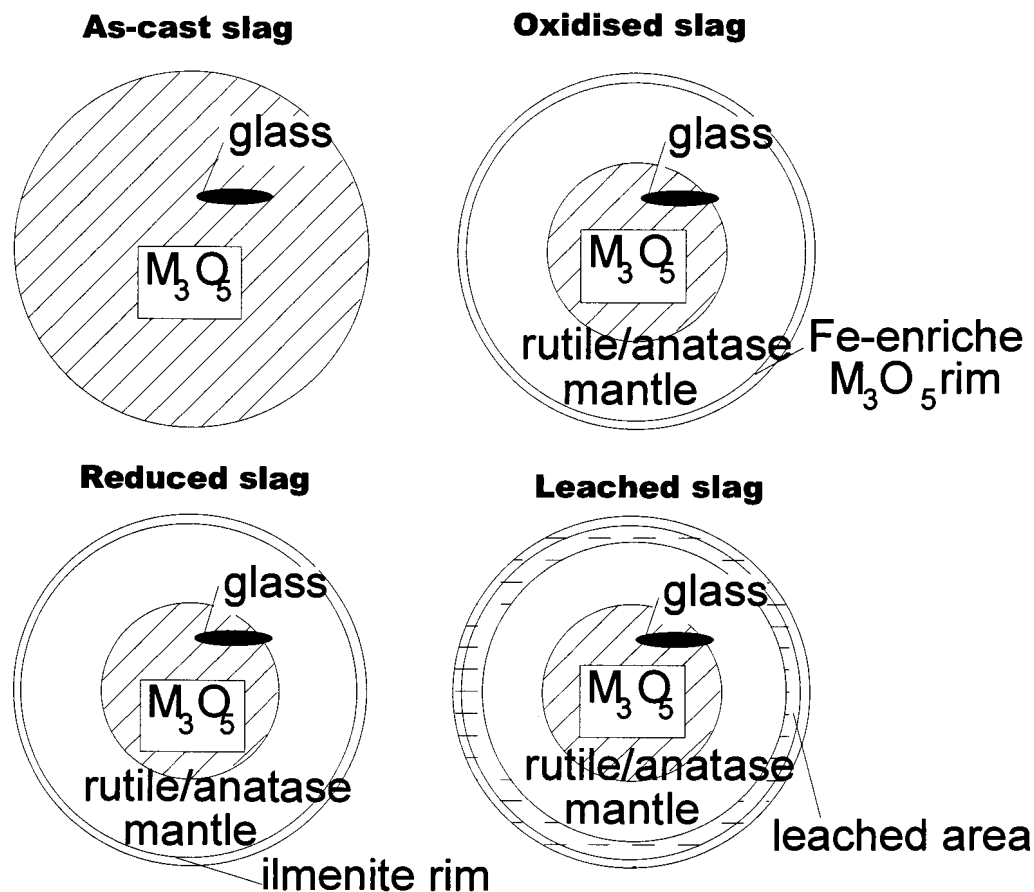
**Figure 25.** Summary of the morphological changes that occur during the production of BTS

Some of the larger slag particles retained unreacted $M_3O_5$ cores after oxidation. Iron migrated to the outside rims of the particles and probably existed as a $M_3O_5$ type solid solution as the XRD results indicated that the $M_3O_5$ phase was still the only iron-containing phase present in the slag. Two distinct phases could be recognised in this zone. From the SEM photographs there appears to be a difference in the iron content of the two phases. The reacted mantles of the particles were porous and consisted of a mixture of rutile and anatase. In the unreacted cores metallic iron precipitates in association with rutile occurred around cracks. Variation of the oxidation time and temperature changed the ratio of anatase to rutile in the slag. With short oxidation times anatase was dominant, while at longer oxidation times rutile became more dominant. Rutile was also dominant at higher oxidation temperatures and with increased oxidation times at the high temperature anatase completely disappeared. At lower oxidation temperatures anatase was dominant but the kinetics of oxidation slowed down significantly. **Reduction** resulted in the formation of ilmenite. The ilmenite formed in the iron-enriched rims on the outsides of the particles. The metallic iron/rutile association was still present in the unreacted cores. Rutile seemed to occur mainly on the outsides of the particles, while anatase dominated in the centres. **Leaching** removed mainly the ilmenite phase. The leached parts of the particles consisted predominantly of rutile, while the un-leached parts consisted of anatase. This observation could have been due to calcination of all the samples prior to analysis. The smaller particles were leached completely and had a "weathered"

appearance. Only the rims of the larger particles were leached and some still had unreacted $M_3O_5$ cores. The metallic iron-rutile association was still present in these cores. The glass phase in all the particles were unaffected by leaching.

### 3.3.4.2 High iron slag

High iron slag by definition contains more than 10 % FeO. In the **as-cast** form the slag consisted mainly of the $M_3O_5$ solid solution phase, but rutile and ilmenite were also present in small quantities. The ilmenite occurred as crystals in a silica glass phase. **Oxidation** of the high iron slag also proceeded in a shrinking core fashion. This led to unreacted $M_3O_5$ cores in the particle centres surrounded by mantles of $TiO_2$. Oxidation resulted in iron migration to the outer rims of the slag particles as well as the edges of cracks extending through the particles. The amount of iron migration seemed to be more than that observed in the standard slag, probably because there was more iron present in the slag. After the oxidation procedure the $M_3O_5$ phase, rutile and anatase occurred as major phases in the slag, while the ilmenite was unaffected. The appearance of the unreacted $M_3O_5$ cores changed to a paler colour during **reduction** and they seemed somewhat smaller than in the oxidised slag. The amount of ilmenite increased from trace quantities to minor quantities as some of the iron in the iron-enriched zones was converted to ilmenite. At the same time the $M_3O_5$ phase decreased from a major phase to a phase that was only present in trace amounts. The slag particles became porous with a "weathered" appearance during **leaching**. The leach procedure removed mainly the ilmenite phase (including the ilmenite in the glass phase) and after 1 h of leaching there was no more ilmenite present in the slag. The leached areas consisted of rutile, while the unleached areas consisted mainly of anatase.

### 3.3.4.3 High magnesia slag

High magnesia slag by definition contains more than 2 % MgO. This slag could result from poor slag making practice when the refractory lining of the slag furnace is eroded or from high MgO levels in the ilmenite feedstock to the slag furnace. The slag in the **as-cast** form also consists of the $M_3O_5$ solid solution phase. The **oxidised** slag had the same zoned appearance as the standard slag with unreacted cores in the particle centres surrounded by a mantle of $TiO_2$. Iron migration also occurred towards the outside rims of the particles and to cracks extending through the particles, but the amount of iron migration was much lower than that observed in the standard slag. At the start of the oxidation procedure anatase and rutile were the dominant phases along with the $M_3O_5$ solid solution. With increased oxidation times rutile became the major phase and anatase and $M_3O_5$ occurred as minor phases. Ilmenite was present as a minor phase after 2 h oxidation, but it disappeared with longer oxidation times. The amount of anatase increased to a main phase during **reduction** and the $M_3O_5$ phase decreased to trace quantities. Ilmenite also formed in the iron-enriched zones at the particle rims. Iron sulphide was picked up in the reduced sample. **Leaching** removed the ilmenite phase.

## 3.4 Conclusions

- The optimum roast conditions are oxidation at 850 °C for 3 h and reduction at 800 °C for 30 min.
- The oxidation roast is the most crucial part of the BTS process as important structural changes occur in the slag during this process stage that influence all the subsequent BTS process stages. These structural changes are the conversion of the original $M_3O_5$ phase to rutile and a new iron rich $M_3O_5$ phase and the migration of iron to the outside rims of the slag particles.
- The effectiveness of the oxidation roast is influenced by the roasting temperature and the chemical composition of the slag.
- High iron and high magnesia slags do not yield BTS of the required grade.
- During oxidation iron migration occurs towards the outsides of the slag particles where reduction converts it to ilmenite. The ilmenite phase is removed during leaching.
- The rate of leaching of iron from the roasted slag is a strong function of hydrochloric acid concentration. The final purity of the BTS product increased slightly with increasing acid strength after extended leaching.
- The rate of leaching is independent of the level of stoichiometric excess hydrochloric acid. The level of stoichiometric excess did not affect the final purity of the BTS product.
- The optimum leaching conditions are 12 h in boiling 20 % HCl at a 20 % stoichiometric excess.
- The highest BTS grade produced was 94 % $TiO_2$.